

Polarisation fields in III-nitrides: effects and control

C. Ren*

III-Nitrides are materials that have revolutionised the lighting industry allowing for the development of high brightness and efficiency white light emitting diodes (LEDs), enabling cost and energy savings at an unprecedented scale. However, there remain several obstacles to the further enhancement of the efficiency of LEDs, particularly for emission at longer wavelengths. The existence of polarisation fields as an inherent material property of wurtzite III-nitride materials severely hampers LED performance. The origin of these fields due to the deviation from an ideal tetrahedral bonding structure and their relation to strain has been addressed in this review. The effect of the polarisation fields on the band structure of heterostructure quantum wells, known as the quantum confined stark effect, and its implications for the efficiency and spectral stability of LEDs have also been reviewed. Finally, the effectiveness and viability of several proposed methods of mitigating the harmful effects of the polarisation fields, such as the growth of III-nitrides on alternative planes, doping, strain engineering and growth of cubic GaN, have been addressed.

Introduction

Gallium nitride (GaN), indium nitride (InN), aluminium nitride (AlN) and their associated alloys are a family of materials known as 'III-nitrides'. This particular branch of the III-V semiconductor family has radically altered the lighting industry due to the high efficiency and brightness of short wavelength III-nitride light emitting diodes (LEDs) and laser diodes. The global push towards efficient lighting has generated considerable interest for materials research in III-nitrides in the past two decades, culminating in the Nobel Prize for physics being awarded in 2014 to S. Nakamura, H. Amano and I. Akasaki for their pioneering work on GaN LEDs.¹ The true breakthrough in lighting with regard to III-nitride LEDs is their ability to emit light brightly and efficiently in the blue to UV spectral range, properties without which it would be extremely difficult to produce white light LEDs. The worldwide replacement of traditional lighting sources such as incandescent bulbs with LEDs, perhaps best highlighted by China's recent ban on traditional lighting sources,² is a clear demonstration of the incredible impact that III-nitrides have had on the world since the demonstration of the first high brightness blue LED.³

Much of the research in III-nitrides since their first implementation in optoelectronic devices two decades ago³ has been focused on mitigating material issues that adversely affect device performance. One of the principal issues is related to crystal quality and originates from the

fact that most GaN films are grown on lattice mismatched substrates due to the high cost of bulk GaN substrates,⁴ resulting in the presence of numerous defects that are detrimental to device performance.⁵ Bennett⁵ has reviewed the somewhat controversial origin of these defects and methods for reducing their density; as such, this review will not focus on this particular issue. Instead, another critical issue that is inherent to the material system will be addressed in this review: III-nitrides are commonly grown along the *c* direction [0001] resulting in the presence of internal polarisation fields along the growth direction that have a devastating effect on LED performance. This work will first review the origin of these polarisation fields and the precise mechanisms through which they hamper LED performance. Following the discussion of the origin and effects of polarisation fields in III-nitride optoelectronics, methods for the mitigation of these effects and their viability will also be reviewed.

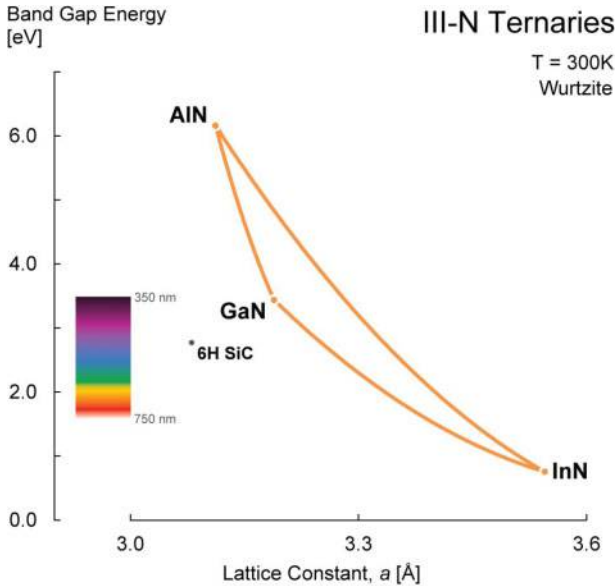
Properties of III-nitrides

III-Nitrides crystallise in two types of crystal structures: hexagonal (wurtzite) and cubic (zinc blende and rock salt). Hexagonal lattice III-nitrides have been the primary subject of academic and industrial investigations as they are more structurally stable under ambient conditions, although there has also been some interest in the study of cubic III-nitrides for LED applications.⁶ III-Nitrides can exist in two polarities, depending on the orientation of the initial layer deposited on the substrate during growth, due to the lack of inversion symmetry in the (0001) plane.⁷

The considerable interest in III-nitrides for optoelectronic applications is primarily due to a large direct bandgap range attainable through alloying, as shown in Fig. 1.

University of Cambridge, Cambridge, UK

*Corresponding author, email christopher.x.ren@gmail.com



1 Bandgap energy against lattice parameter for III-nitrides at 300 K (Ref. 8)

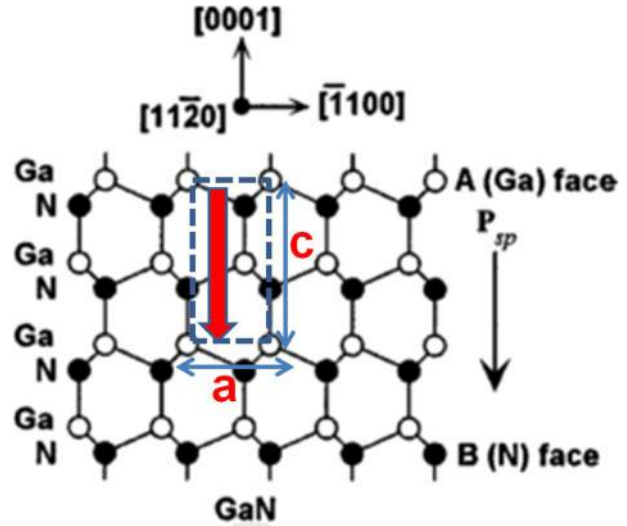
The bandgaps attainable through alloying are represented by the solid lines connecting the end members. The direct bandgap of III-nitrides is a vital property in their application in photonic devices as this allows for the efficient absorption and emission of photons without the need for phonon interactions. There is considerable interest in the use of III-nitride materials for optoelectronic applications, as they can, in theory, be designed to emit and absorb light across the entire visible, infrared and ultraviolet ranges.

III-Nitrides are most commonly grown by metal-organic vapour phase epitaxy (MOVPE)⁵ but are also grown using halide vapour phase epitaxy (HVPE), molecular beam epitaxy and reactive sputtering.⁹ Most III-nitride films are grown on foreign substrates (heteroepitaxially) due to the high production cost of bulk GaN substrates.⁴ Silicon, silicon carbide and sapphire are all used as substrates for the growth of III-nitrides, although all exhibit a lattice mismatch with III-nitrides, resulting in issues with crystal quality.⁴

Polarisation fields in III-nitrides

III-Nitride materials in wurtzite form are known as polar materials, which means that they exhibit spontaneous polarisation without the presence of an external electric field.¹⁰ The orientation of the spontaneous polarisation is along the $[000\bar{1}]$ direction and thus can only be manipulated by changing the polarity (Ga/N polar) of the GaN. The origin of this spontaneous polarisation is the deviation from an ideal tetrahedral coordination along the (0001) axis for the III-nitride wurtzite crystal and the ionicity of the crystal (the difference in respective electronegativities of the two elements forming a bond).¹¹ As a result of these conditions, each unit cell exhibits a non-zero dipole moment in the $[000\bar{1}]$ direction, as shown schematically in Fig. 2.

This effect is particularly pronounced for III-nitrides compared to other III-V semiconductors as nitrogen is the most electronegative and smallest group V element, resulting in a metal-nitrogen bond with far greater ionicity than other III-V bonds.¹³



2 Crystal structure for GaN, with unit cell (blue dashed line), dipole moment (red arrow) and lattice parameters a and c denoted in red¹²

For an ideal hexagonal closed packed crystal with zero spontaneous polarisation, the ratio of the lattice parameters c_0 and a_0 , if all nearest neighbour bond lengths are equal as denoted in Fig. 2, is given by

$$\frac{c_0}{a_0} = (8/3)^{1/2} = 1.63299$$

Thus, for non-ideal structures with a c/a ratio that deviates from the ideal value, a spontaneous polarisation appears. The bulk c/a ratio for each III-nitride compound is shown in Table 1.

As the c/a ratio decreases, the angle between the three bonds at the base of the tetrahedral bonding structure increases, resulting in a lower compensation polarisation along the c -axis and an enhanced spontaneous polarisation.¹³ As shown in Table 1, the strongest spontaneous polarisation is observed in AlN and the weakest in GaN.

Materials that exhibit spontaneous polarisation also exhibit a piezoelectric polarisation.¹⁰ Any strain experienced by the crystal will distort the crystal lattice, in some cases further exacerbating the deviation from an ideal c/a ratio and resulting in the presence of an additional polarisation.

The piezoelectric polarisation is an important consideration when evaluating polarisation fields in III-nitrides as most films are grown heteroepitaxially and devices are typically heterostructures: in-plane lattice constant mismatches with the underlying layer result in the expansion or contraction of the III-nitride film. Biaxial compressive stress results in a decrease of the in-plane lattice parameter a and an increase in the vertical lattice parameter c , returning the c/a ratio towards its ideal value and thus resulting in a piezoelectric polarisation that opposes the spontaneous polarisation. On the other hand, if tensile stress is applied in the c direction, the c/a ratio is lowered, and the overall polarisation is increased as the spontaneous and

Table 1 Bulk c/a ratios for AlN, GaN and InN

Material	AlN	GaN	InN
c/a	1.6010	1.6259	1.6116

piezoelectric components now act in the same direction.¹³ This interestingly results in two different polarisation configurations for the two common ternary alloys of GaN (AlGaN and InGaN) when coherently strained to GaN. In the case of InGaN, the piezoelectric field actually acts against the spontaneous field, whereas with AlGaN the piezoelectric field acts in the same direction.

Light emitting diodes: basics and operation

Light emitting diode structures for visible light application typically use InGaN/GaN quantum wells (QWs) for the active region. A general LED structure is shown in Fig. 3.

The structure typically contains a magnesium doped p type region containing free positive carriers and a silicon doped n type region containing free electrons. In order to avoid the leakage of electrons into the p-GaN region, AlGaN (a material with a higher bandgap than GaN) is used as an electron blocking layer.

The active region, composed of QWs formed by alternating InGaN and GaN layers, captures the carriers that recombine to emit photons. Carriers can also combine non-radiatively through the emission of a phonon rather than a photon. Phonons are essentially quantised lattice vibrations, or heat, and negatively affect the performance of the LED in addition to quenching light emission. Owing to their nature as charged particles, electrons and holes in the QWs can be bound by Coulombic attraction to form charge neutral quasi-particles known as excitons. These excitons can

decay to emit light, albeit at an energy slightly lower than for free carriers due to their original binding energy.

Light emitting diode active regions: QWs

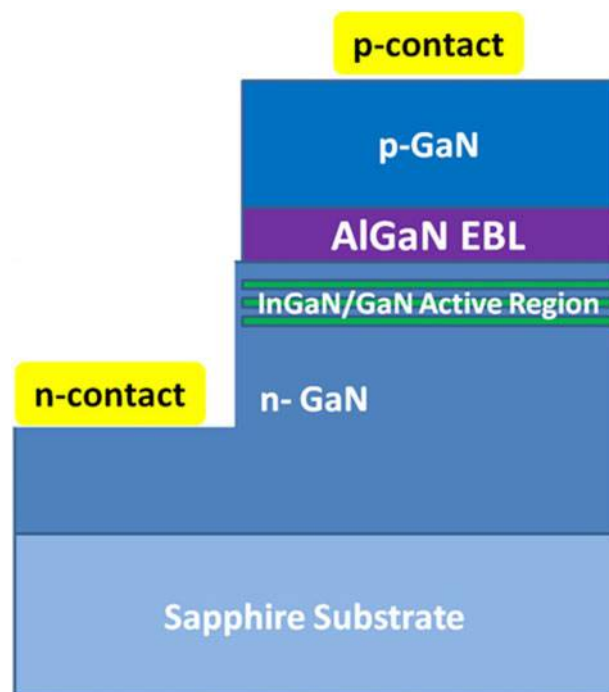
The first successful III-nitride LED consisted, in its entirety, of a p–n junction of a single material, known as a ‘homojunction’.¹⁴ However, LED structure designs have since moved on and are now primarily composed of heterostructures known as QWs.

Quantum wells are composed of a thin layer of low bandgap material, typically on the order of several nanometres, in between two high bandgap quantum barriers (QBs). This results in the confinement of carriers in the low bandgap region in one direction, hence the term ‘quantum well’. This quantum confinement leads to the discretisation of carrier wave functions within the well.

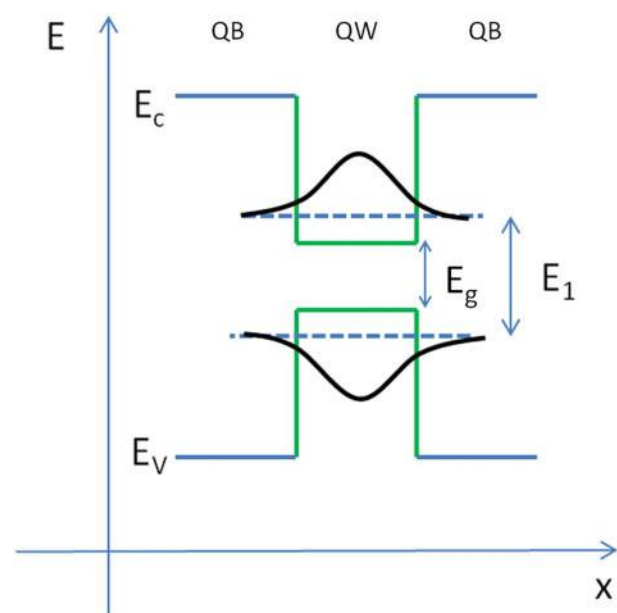
Two effects arise from this confinement with regard to optoelectronic devices: the carrier recombination probabilities and thus the efficiency of the device is enhanced and the emission wavelength of the structure is blue shifted relative to the emission of the bulk material due to the introduction of bound states.¹⁴

In a typical LED structure, the QW is positioned between the p and n doped regions of the device, allowing it to capture carriers flowing from one side to another under the application of a forward bias.

For III-nitride LEDs emitting in the blue region of the visible spectrum, GaN is typically alloyed with In at mole fractions of around 10–20% to achieve an appropriate bandgap for the QW region, with the QBs consisting of GaN.¹⁵ While QWs are typically schematically illustrated as having abrupt interfaces, it should be noted that typical compositional profiles are not square,^{16–19} and hence, deviations from the potential profile illustrated in Fig. 4 occur. Equally, the challenges of growing these very thin layers may mean that in a multiple QW



3 Visible light LED structure on a sapphire substrate. A forward bias applied to the structure through the metallic contacts at the p and n regions causes electrons from the n-GaN and holes from the p-GaN to flow towards the active region, these carriers then recombine to generate light. The AlGaN electron blocking layer (EBL) serves to stop electrons from entering into the p-type region



4 Energy-band diagram of a quantum well. The conduction and valence band edges are denoted E_c and E_v respectively. The bandgap of the well material is denoted E_g and the energy of the ground state transition is denoted E_1

structure, while the intended structures have constant composition and thickness, variations throughout the QW stack may occur.¹⁷

Quantum confined stark effect in III-nitrides

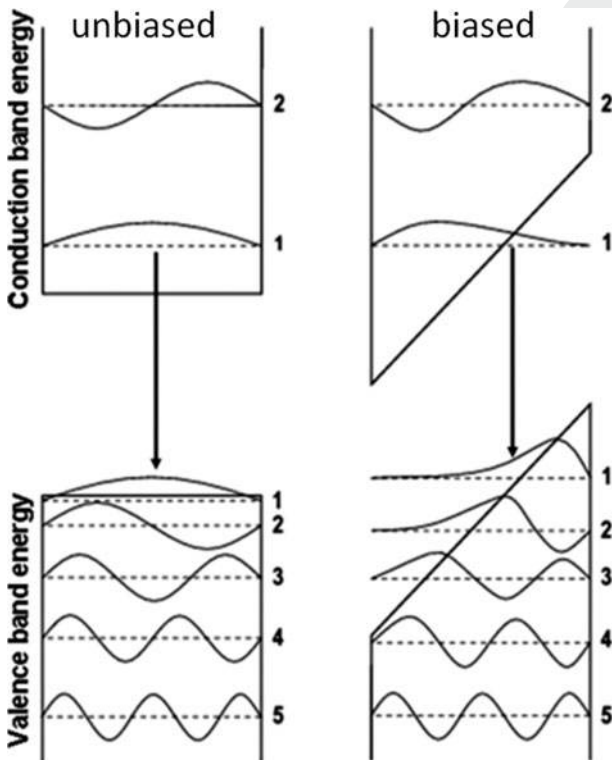
The origin of the quantum confined stark effect (QCSE) was first reported by Miller *et al.* for aluminium gallium arsenide (AlGaAs) QWs based on the observation that electric fields applied perpendicular to the QW layers resulted in large red shifts in absorption.²⁰ The mechanism behind this shift is illustrated in Fig. 5.

The applied potential changes the QW from a rectangular to a 'sawtooth' shaped well, resulting in the reduced overlap of the electron and hole wave functions as they are pushed in opposite directions.

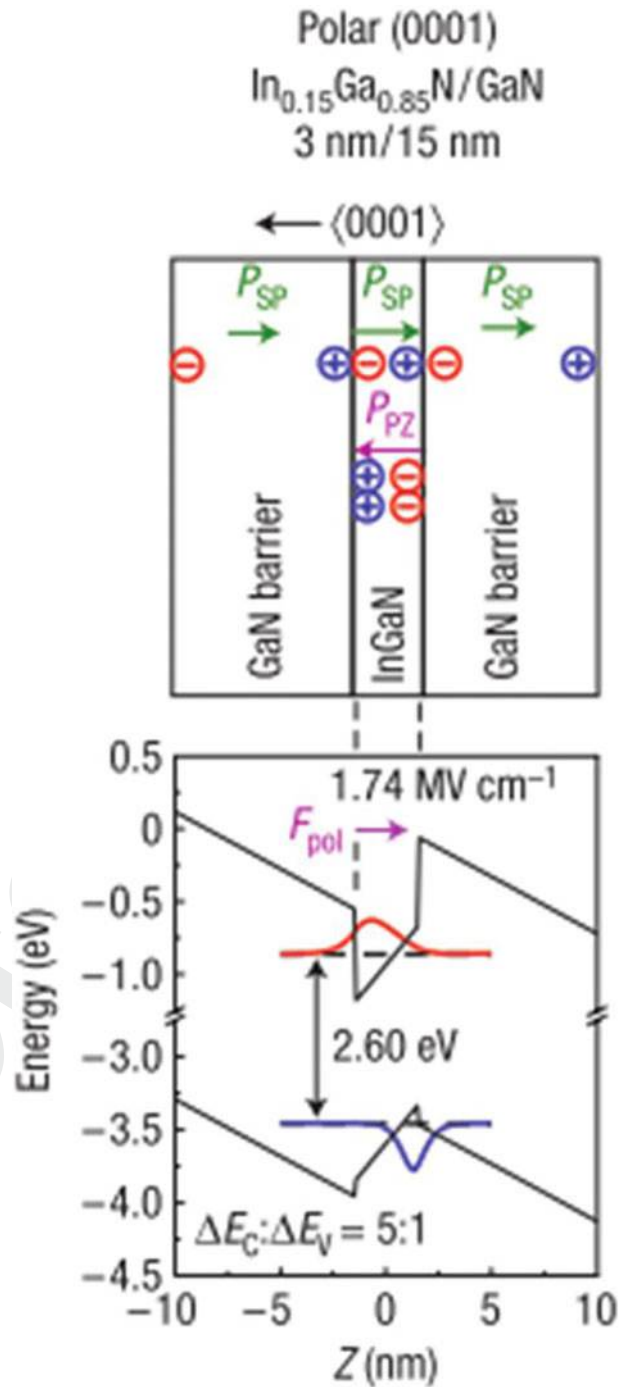
In the context of III-nitride LEDs, it is important to consider the spontaneous and piezoelectric contributions to the overall QSCE. In the case of InGaN/GaN heterostructures for visible light LEDs, the QSCE is dominated by the piezoelectric contribution²² to polarisation fields due to the large lattice mismatch between GaN and InN (~11%).²³ The compressive strain experienced by a 3 nm InGaN QW between two 15 nm GaN QBs and the consequent piezoelectric polarisations are illustrated in Fig. 6.

Polarisation effects in LED devices

The following sections will focus on the characterisation of polarisation induced effects on the optoelectronic properties of III-nitride heterostructures rather than their direct measurement through methods such as electron holography, which have previously been



5 Quantum well energy levels for unbiased and biased structure with carrier wave functions for different energy levels;²¹ applied bias reduces overlap between carrier wave functions



6 Illustration of polarisation fields and band profile for $\text{In}_{0.15}\text{Ga}_{0.85}\text{N}/\text{GaN}$ QW; note tilted bands of both QW and QBs due to polarisation fields; polarisation charges appear at interfaces due to spontaneous polarisation P_{sp} and piezoelectric polarisation P_{pz} (Ref. 14)

demonstrated for various structures such as InGaN QWs,^{24,25} AlGaIn/GaN/InGaIn diodes²⁶ and at dislocation cores.^{27,28}

Bandgap narrowing and power dependent emission blue shift

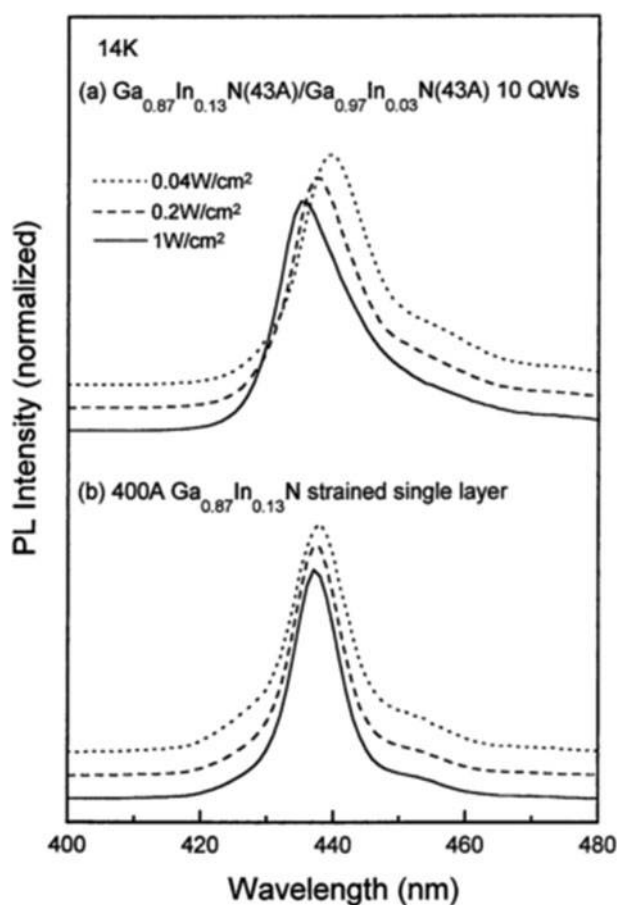
The spatial separation of the carriers in a triangular QW has several consequences on the emission properties of the LED. In this section, we will discuss how the rhombic or 'sawtooth' shape of the QW results in the energy of the optical transition being reduced, which is

known as bandgap narrowing that causes a red shifted emission wavelength.

The majority of early experiments reporting the effects of bandgap narrowing in III-nitrides consisted of photoluminescence (PL) experiments, whereby carriers are generated using incident illumination and recombine to emit light. As the bandgap narrowing effect is due to the polarisation fields present in nitrides, it stands that the presence of carriers effectively nullifies this effect by screening the culpable electric fields. The effects of the QCSE in III-nitride QWs were first reported by Takeuchi *et al.*²⁹ The authors compared the PL spectra of a structure containing multiple InGaN QWs with those of another structure consisting of a single bulk InGaN layer with increasing illumination power. The results are shown in Fig. 7.

The blue shift experienced by the QW structure indicates the screening of the polarisation fields by carriers generated by the incident light.³⁰ The original peak emission wavelength of the QW structure is initially red shifted relative to the bulk InGaN epilayer due to the tilting of the QW energy bands, which results in bandgap narrowing due to the piezoelectric field²⁹ as shown in Fig. 7.

Although power dependent measurements are an effective way of probing the effects of bandgap narrowing, an equally useful way is to examine the time dependence of the effects of carrier screening. Kim *et al.* used this approach by employing time resolved PL



7 Photoluminescence spectra of *a* multiple QW structure and *b* single InGaN layer with increasing excitation power; spectra for QW structure exhibit blue shift in peak emission wavelength with increasing excitation power, while bulk layer spectra remained largely unchanged²⁹

spectroscopy to study the QCSE and the effect of carrier screening in GaN–AlGaIn QWs. By taking PL spectra at different delay times after an initial picosecond excitation pulse, the authors observed a substantial red shift in peak emission wavelength with increasing delay, indicating a ‘recovery’ of the original QCSE in the QWs after initial screening by photoexcited carriers as shown in Fig. 8.³¹

As an alternative to carrier bandgap screening through power or time dependent PL experiments, it has been shown that electrically contacting and biasing III-nitride LED structures is perhaps a more direct method of evaluating the effect of the piezoelectric fields on bandgap narrowing as it no longer relies on the injection of carriers for field screening but instead directly affects the tilting of the band structure. Takeuchi *et al.* used this approach and examined electrically contacted p–i–n InGaIn–GaN QW structures. Photoluminescence spectra at increasing reverse bias were examined with an enhanced blue shift observed.³² The results are shown in Fig. 9.

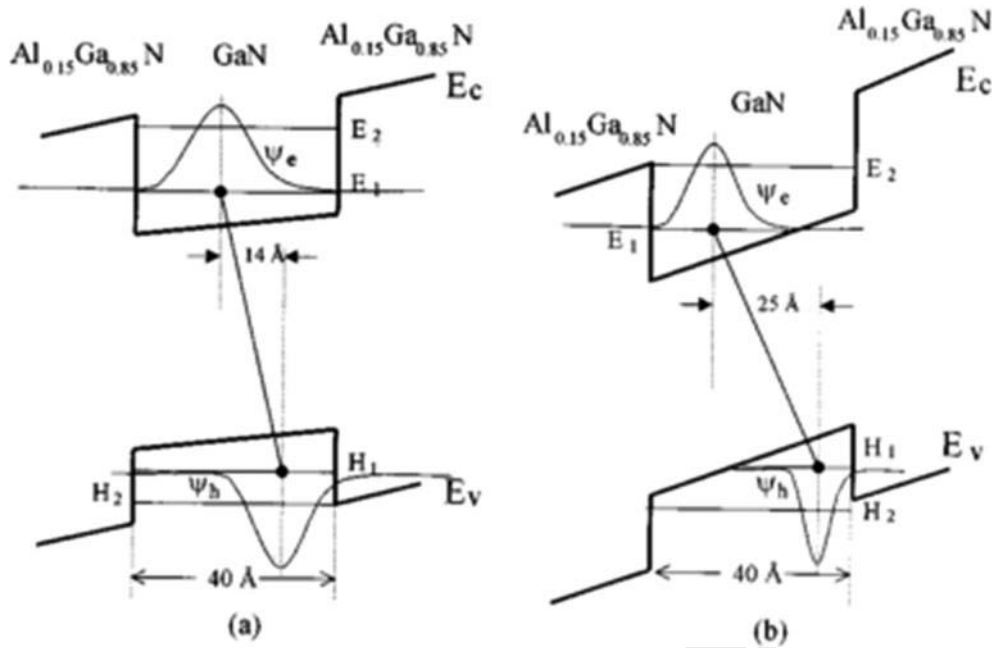
The observed relationship between peak emission blue shift and increasing reverse bias can be interpreted by considering the effect of the reverse bias on the energy bands of the QW. A reverse bias actually serves to tilt the energy bands of the QW towards the so called ‘flatband condition, where the influence of the piezoelectric effect has been nullified.³² As a result, the reverse bias causes blue shift in the QW emission energy.

Given the aim of LEDs is to produce light under electrical bias, or electroluminescence (EL), it is important to consider the effect of electrical injection on the polarisation fields. Epitaxial structures for III-nitride based LEDs are typically grown with the p type layer last due to well documented difficulties with p type doping^{33–36} and thus function under forward bias conditions. Interestingly, the application of a forward bias should have the opposite effect on the QW energy bands to the one observed by Takeuchi *et al.*³² if one ignores the effects of carrier screening. On the contrary, increasing the forward bias on a p–i–n InGaIn–GaN QW LED structure results in a blue shift in the peak EL spectrum for III-nitride layers grown along the [0001] direction.³⁷ This blue shift is attributed to the same effect observed for PL under increasing excitation power:²⁹ increasing bias allows for the injection of a greater number of free carriers into the QW, which in turn result in the partial screening of the QCSE inducing a blue shift in peak emission wavelength.²¹

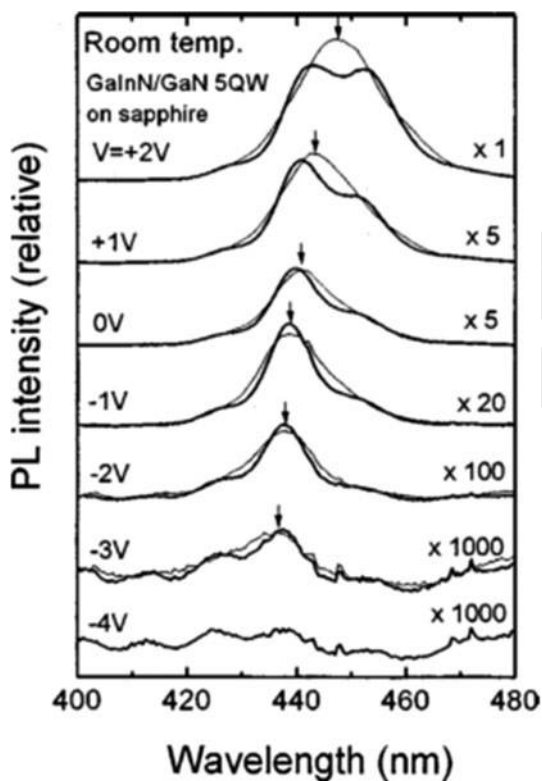
Reduction in oscillator strength and efficiency

The spatial separation of carriers due to the polarisation fields in III-nitride heterostructures results in a decreased probability for radiative recombination or a reduction in oscillator strength. The concept of oscillator strength expresses the probability of interaction between the energy levels of a system and electromagnetic radiation. In essence, the oscillator strengths for a QW determine its emission and absorption properties:³⁸ the stronger the oscillator for a particular transition, the more likely it is to occur.³⁹ The oscillator strength of a system can be experimentally inferred as it is directly related to the rate of luminescence decay: a strongly emitting oscillator results in fast decay of the luminescence due to the high transition probability.

As we have noted in the previous section, the effect of the QCSE from the polarisation fields in III-nitride QWs



8 Energy band diagrams of GaN- $\text{Al}_x\text{Ga}_{1-x}\text{N}$ QW *a* under influence of screening by photogenerated carriers at time $t_d = 0$ and *b* after long delay time, returning to original piezoelectric field that causes increased tilting of QW bands and increased spatial separation of carrier wavefunctions³¹



9 Photoluminescence spectra of $\text{In}_{0.16}\text{Ga}_{0.86}\text{N}/\text{GaN}$ p-i-n structure with increasing reverse bias; thin lines represented data fitted to remove interference fringes, and raw data are denoted by thick lines; under reverse bias, p-i-n structure is more likely to generate photocurrent upon illumination rather than subsequent PL, hence dramatic reduction in PL intensity; peak positions of spectra are shown by arrows³²

is to transform the QW into a triangular potential and thus spatially separate the electron and hole

wave functions. This is exacerbated for thicker wells, as demonstrated in Fig. 10.

This effect was used by Im *et al.* to examine the reduction of oscillator strength in AlGaIn/GaN.⁴⁰ Thicker wells were first observed to have higher peak emission wavelength relative to the GaN bandgap, an indication of the bandgap narrowing effect previously discussed. The luminescence lifetime of the red shifted emission from the thickest well (10 nm) was observed to be 3 μs , a factor of 10^4 longer than the decay times for the thinner wells.

Chichibu *et al.* reported similar effects for InGaIn-GaN QWs of varying thickness, noting that the decay times for PL were strongly QW thickness dependent⁴¹ as shown in Fig. 11.

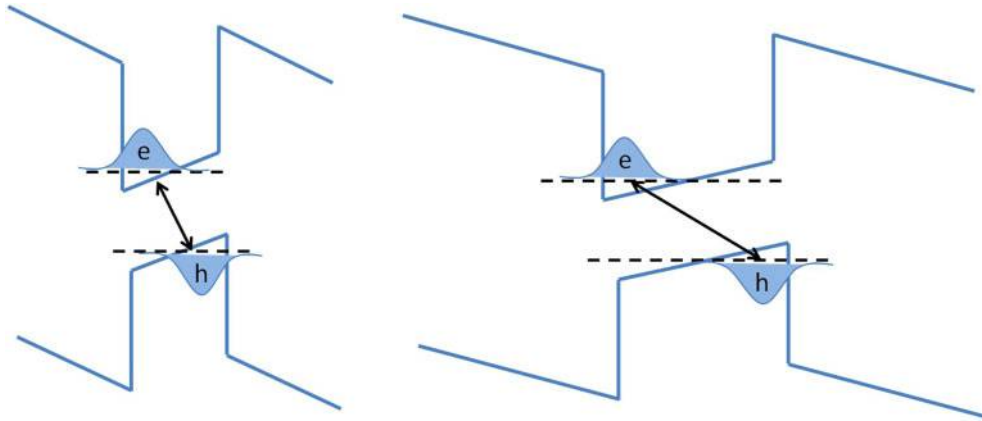
The reduction in oscillator strength has significant consequences in terms of LED device efficiency. Radiative and non-radiative processes are in competition; thus, if the radiative lifetime is increased, free carriers are far more likely to recombine non-radiatively at defects.⁴² This severely hinders LED device efficiency, particularly in the long wavelength spectral ranges as will be discussed later.

The issue of efficiency 'droop' or the fall-off of III-nitride LED efficiency can also be related to this reduction in oscillator strength. Although the origin of efficiency droop is disputed,⁴³⁻⁴⁵ it is clear that it occurs for increasing injection carrier density. As such, it would be desirable to grow LED devices with wider QWs in order to reduce carrier density in the wells during operation and thus alleviate the efficiency droop.⁴⁶ However, the presence of thicker wells would cause even further separation between carriers in the case of polar LEDs, reducing the radiative recombination probability and thus device efficiency even further.

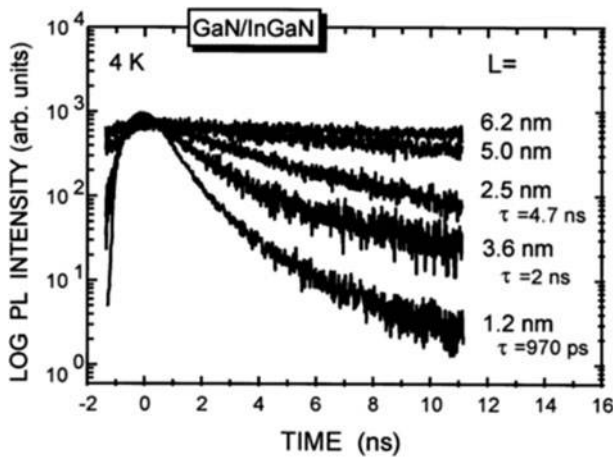
Mitigating the QCSE

Alternative growth planes

One method to circumvent the deleterious effects of internal fields in III-nitride heterostructures is to redirect



10 Thicker QWs in III-nitrides result in larger spatial separations of electrons and holes and reduced oscillator strength



11 Time resolved PL decay curves for varying well thickness; 5.0 and 6.2 nm thick QWs showed decay lifetimes far beyond range of x-axis;⁴¹ it is clear that thinnest well exhibits fastest decay time and thus highest oscillator strength

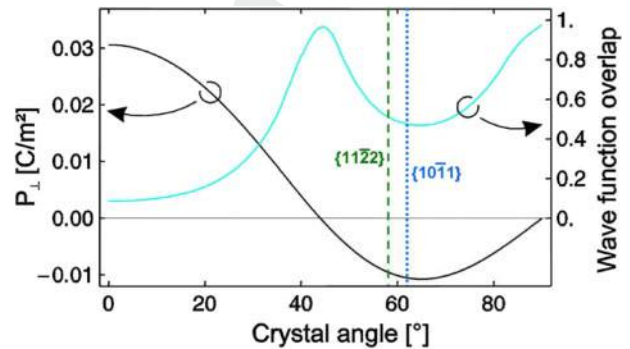
the biaxial stress (which is responsible for the piezoelectric polarisation field) along another crystal plane.⁴⁷ The electric field vanishes entirely for facets perpendicular to the {0001} plane (*c* plane) such as the {11 $\bar{2}$ 0} or {10 $\bar{1}$ 0} planes (*a* and *m* planes respectively).

The relationship between crystal angle relative to the *c* plane, piezoelectric polarisation and carrier wave function overlap for a 3 nm thick In_{0.25}Ga_{0.75}N QW pseudomorphically strained to the GaN QBs is illustrated in Fig. 12.

The *a* and *m* planes are thus denoted as 'non-polar' due to the vanishing polarisation fields along the growth direction. Alternative GaN growth orientations are shown schematically in terms of a GaN unit cell in Fig. 13.

a plane growth

a plane GaN is almost exclusively grown by MOVPE. The most commonly used substrate is *r* plane sapphire due to its readily available nature and its well established epitaxial relationship with GaN.⁴ The low crystal quality of *a* plane GaN grown by MOVPE remains one of the primary obstacles to establishing *a* plane GaN as a viable non-polar alternative to *c* plane GaN for LED devices.⁴⁹ Typical values of stacking fault densities and dislocation densities are in the range of $5 \times 10^5 \text{ cm}^{-1}$ and 10^9 cm^{-2} respectively. On the other hand, dislocation

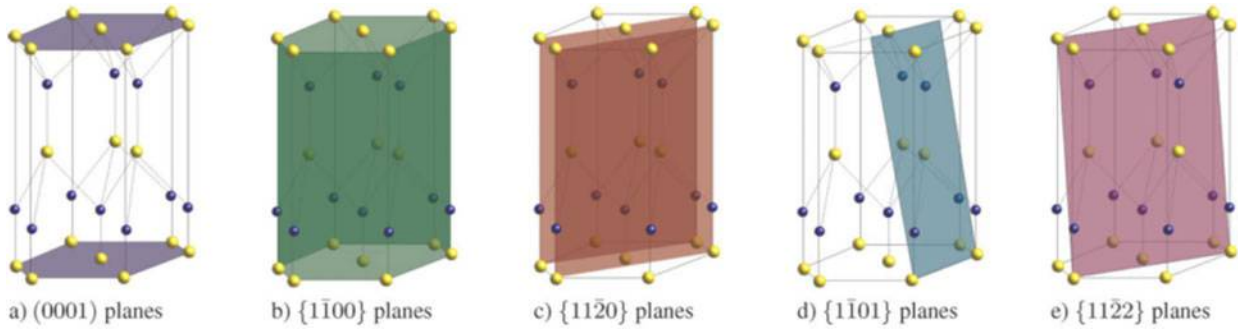


12 Piezoelectric polarisation (right axis/black curve) and relative carrier wavefunction overlap (left axis/black curve) for 3 nm thick InGaN QW with respect to crystal angle relative to *c* plane; semipolar planes are shown by dashed line at angle of $\sim 60^\circ$ (Ref. 4)

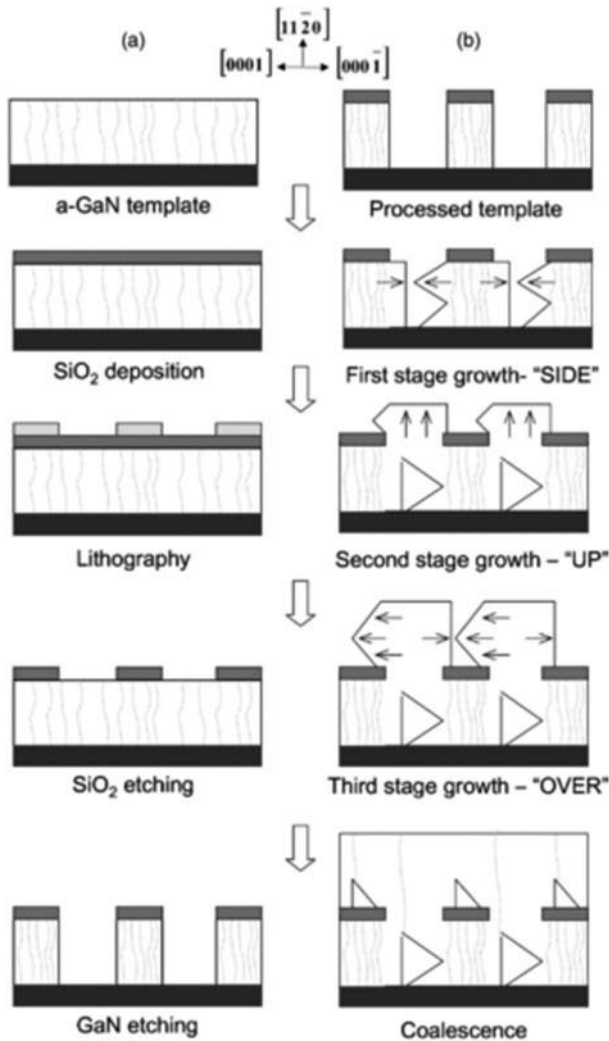
densities on the order of 10^8 cm^{-2} are easily achievable for *c* plane GaN, with even lower values achievable using defect reduction techniques.^{5,50} Stacking faults are less of an issue in *c* plane GaN as they lie perpendicular to the growth direction and can be overgrown by fault free material.⁴ Techniques such as the use of low temperature GaN⁵¹ and high temperature AlN nucleation layers⁵²⁻⁵⁴ have shown fruitful results in the case of improving polar III-nitride growth. Similar approaches have also resulted in some limited improvements to *a* plane GaN layer qualities.⁵⁵ However, the technique yielding the greatest improvement in material quality is epitaxial lateral overgrowth (ELOG), as shown schematically in Fig. 14.

In the SLEO process, a GaN buffer layer is first grown and covered with a dielectric mask, which is then patterned using optical lithography. As the epitaxial growth is continued, the GaN grows laterally (along the [0001] direction) out of the defined openings and coalesces. This method results in a considerable reduction in defect densities in the epitaxial film.

Early attempts at growing *a* plane LED devices were plagued by the effects of large defect and stacking fault densities. Chitnis *et al.* reported a slow turn-on for an *a* plane GaN-InGaN QW LED structure, most likely due to the presence of dislocations and stacking faults as leakage conduction pathways.⁵⁷ Using an ELOG approach and low defect density HVPE grown templates, Chakraborty *et al.* produced *a* plane LED



13 GaN surface orientations: *a c* plane, *b m* plane, *c a* plane, *d* and *e* semipolar planes; gallium atoms in yellow and nitrogen in blue⁴⁸



14 Sidewall epitaxial overgrowth (SLEO) process for *a* plane GaN⁵⁶

structures with improved current-voltage characteristics, with relatively intense emission at a peak wavelength of 413 nm independent of drive current, as expected of non-polar LED structures.⁵⁸

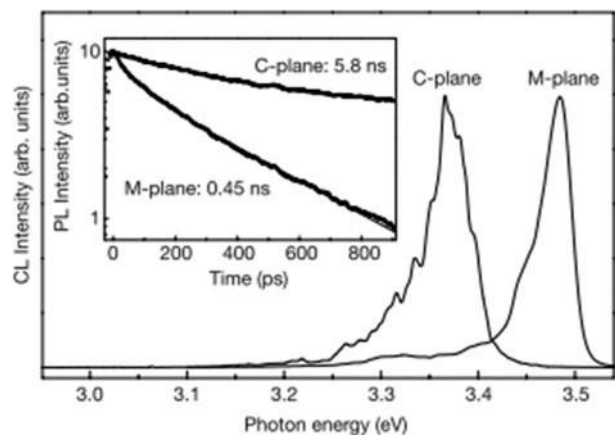
Rather ironically, *a* plane LED devices for emission at longer wavelengths are particularly afflicted by material quality issues as reduction of the bandgap narrowing effect requires the incorporation of higher indium compositions within the QWs to achieve longer wavelength emission.⁴ This is even further exacerbated by the

apparent inefficient incorporation of indium into *a* plane GaN relative to the *c* plane layers⁵⁹ and semipolar facets in surface pits.³⁹ As such, *a* plane growth is considered suboptimal for the development of high performance LEDs despite its nature as a non-polar solution.⁴⁹

m plane growth

In terms of III-nitride, crystal quality growth along the *m* plane is considered far more promising than that along the *a* plane.⁴ Waltereit *et al.* reported the first instance of an *m* plane AlGaIn/GaN LED structure grown by rf plasma assisted molecular beam epitaxy on a tetragonal LiAlO₂ (LAO) substrate, demonstrating both a decreased luminescence decay lifetime and a luminescence blue shift relative to a *c* plane QW structure of the same well width as shown in Fig. 15 (Ref. 14).

LAO has been considered a favourable candidate for the growth of non-polar III-nitrides due to its small lattice mismatch with *m* plane GaN (0.3–1.7% depending on the direction).⁶¹ Mauder *et al.* also reported promising results in the form of extremely low stacking fault densities for MOVPE grown *m* plane GaN on LAO;⁶¹ however, it has been observed that the high growth temperatures and ambient hydrogen characteristic of MOVPE growth induce damage to the LAO substrate, resulting in large background carrier concentrations, rough surfaces and broad PL emission



15 Cathodoluminescence spectra of *c* plane and *m* plane QW structures; inset shows luminescence decay curves; *m* plane QW structure is both blue shifted and exhibits stronger oscillator strength and thus faster luminescence decay, as expected for non-polar structures¹⁴

spectra,⁶¹ all undesirable features for LED growth. It has been hypothesised that substrate damage is the direct cause for the poor performance of *m* plane LED structures grown by MOVPE on LAO.⁶²

As an alternative, *m* plane silicon carbide (SiC) has also been considered as a substrate for *m* plane growth of GaN. However, as is typical of the heteroepitaxial growth of non-polar GaN, large stacking fault densities ($\sim 10^6 \text{ cm}^{-2}$) have been reported for the growth of *m* plane GaN on SiC, thus requiring the need for techniques such as graded AlGaIn layers⁶³ or SLEO to reduce defect densities.⁶⁴ It should be noted that lateral epitaxial overgrowth techniques are considered effective in reducing threading dislocation density but are far less effective for stacking faults for non-polar growth of GaN.^{65,66}

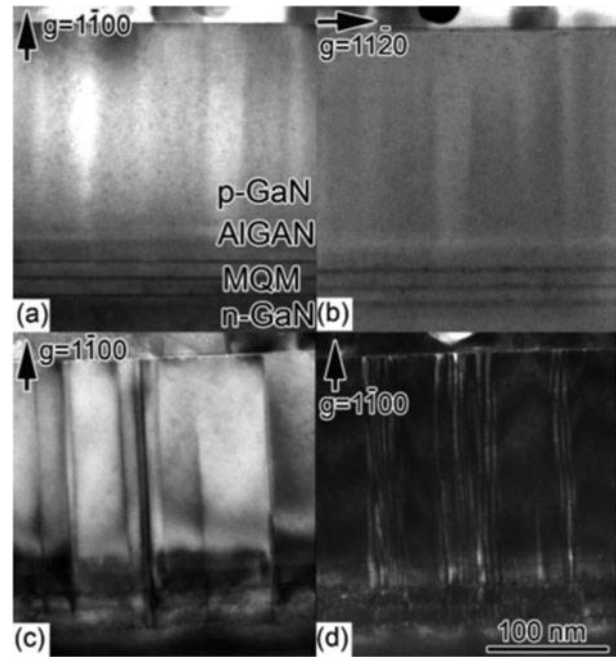
The introduction of bulk GaN crystals grown by HVPE for non-polar growth marks a turning point in the development of non-polar LEDs. III-Nitride QW structures grown on foreign substrates had until then demonstrated large defect densities, even with the use of ELOG techniques, resulting in particularly poor LED device performance with output powers an order of magnitude (below 1 mW at 20 mA drive current) weaker than high performance *c* plane devices.⁴⁹ Okamoto *et al.* demonstrated the first milliwatt level blue *m* plane LEDs by growing the structures on HVPE GaN substrates cut towards the *m* direction.⁶⁷ Shortly thereafter, non-polar growth on cut free standing bulk GaN substrates was used to produce *m* plane LEDs emitting at 407 nm with an output power of 23.7 mW at 20 mA.⁶⁸

Despite the reduction of extended defects in *m* plane GaN through the use of free standing HVPE bulk substrates for growth, device performance beyond the emission wavelength of 500 nm remains hindered by issues with indium incorporation.⁴⁹ Detchprohm *et al.* reported a difference in output power close to two orders of magnitude between *m* plane LED structures emitting at 490 and 510 nm.⁶⁹

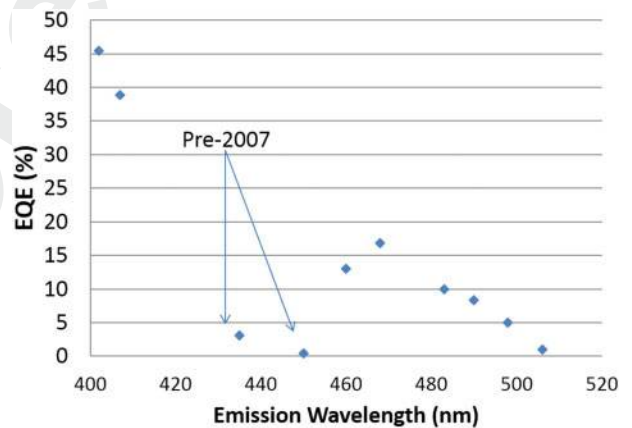
The origin of the dramatic drop in output power with increasing peak emission wavelength has been attributed to the presence of basal plane stacking faults (BSFs) bounded by partial dislocations known as type I₁ BSFs by Wu *et al.*⁷⁰ These partial dislocations act as non-radiative recombination centres, hindering light emission from the LED structure. Transmission electron microscopy (TEM) images were taken for two QW widths (2.5 and 4 nm) for which the corresponding LEDs showed an order of magnitude difference in light output power at 20 mA injection current⁷¹ and demonstrated a clear difference in dislocation and stacking fault densities as shown in Fig. 16.

Furthermore, Wu *et al.* demonstrated that the BSFs and partial dislocations originated from the InGaIn QWs in the structure and not from the substrate, where the dislocation density was far lower than the density calculated from the TEM images.⁷⁰

As such, while *m* plane growth remains far more promising than *a* plane in terms of non-polar LED structures, material issues such as the generation of BSFs and partial dislocations tend to persist when longer emission wavelengths are targeted. Figure 17 demonstrates that the highest EQEs have been achieved for *m* plane devices in the blue spectral range. Although it is unlikely that *m* plane will compete directly with *c* plane LEDs in this range,⁷⁵ reports of reduced efficiency



16 Cross-sectional TEM images along two diffraction conditions for 2.5 nm thick QW LED structure (top left and right), *c* bright field TEM image, and *d* dark field image for 4 nm thick QW; stacking faults and dislocations can easily be observed for 4 nm thick QW sample⁷⁰



17 *m* plane LED external quantum efficiencies (EQEs) against emission wavelength; drop at ~ 500 nm is due to deteriorating quality of *m* plane InGaIn films (from Refs. 67, 68, 71–73); two lowest efficiencies were before development of high quality bulk GaN substrates in 2007 (Ref. 74)

drop at large injection current for *m* plane LEDs relative to *c* plane devices indicate that *m* plane devices may be successful as high efficiency devices at high drive currents.⁷⁶ However, the requirement for expensive bulk cut HVPE grown GaN templates for acceptable crystal quality remains a hindrance in terms of the commercial and industrial viability of non-polar LED growth.

Semipolar growth

Interest in semipolar growth orientations has stemmed from the apparent ~ 500 nm emission wavelength limitation for *m* plane devices. Semipolar III-nitride heterostructures have also been shown to exhibit reduced

internal fields relative to c plane heterostructures⁷⁷ and hence represent a compromise between the deleterious effects of polarisation fields in polar heterostructures and BSF formation in long wavelength non-polar devices.⁴⁹

Initial efforts for growth of GaN on m plane sapphire resulted in twinned growth along the $\langle 10\bar{1}3 \rangle$ direction.⁷⁸ It was subsequently found that sapphire nitridation⁷⁹ and optimisation of temperature and pressure during growth⁸⁰ are crucial to suppress twinned $\langle 10\bar{1}3 \rangle$ growth and favour $\{11\bar{2}2\}$ GaN growth, resulting in smoother surfaces.⁸⁰ Johnston *et al.* demonstrated the use of a scandium nitride (ScN) layer in improving $\{11\bar{2}2\}$ GaN crystal quality by reducing dislocation and BSF densities,⁸¹ a technique already known for c plane growth on r plane sapphire.⁸² In the case of $\{11\bar{2}2\}$ GaN, lateral overgrowth techniques have also been shown to improve crystal quality by reducing stacking fault density.⁸³

The first demonstration of a semipolar InGaN/GaN LED was reported by Kamiyama *et al.*, with a reduced blue shift in peak emission wavelength with increasing injection current relative to a reference c plane LED structure observed.⁸⁴ Following this, Chakraborty *et al.* produced the first semipolar LEDs on free standing $\{10\bar{1}1\}$ and $\{10\bar{1}3\}$ HVPE GaN templates that exhibited drive current independent peak emission wavelength at 439 nm (blue).⁸⁵ As was the case with non-polar LED structures, the performance of semipolar LEDs was greatly enhanced through the use of substrates cut from bulk c plane GaN grown through HVPE.^{86–90}

The apparent higher indium incorporation of the $\{11\bar{2}2\}$ plane relative to the m plane has enabled the growth of LED structures in the green (516 nm)⁹¹ and yellow (562.7 nm)⁹² spectral ranges, a feat unattainable using m plane growth due to the formation of BSFs. The origin of the higher indium incorporation has been reported to be the reduced strain-repulsive interactions of indium atoms in GaN on the $\{11\bar{2}2\}$ plane relative to the m plane.⁹³

Presently, semipolar growth along the $\{20\bar{2}1\}$ and $\{20\bar{2}\bar{1}\}$ planes has yielded the most promising results in terms of long wavelength device performance.⁴⁹ It has been demonstrated that indium incorporation along the $\{20\bar{2}\bar{1}\}$ plane is particularly efficient relative to other non-polar and semipolar facets; furthermore for $\{20\bar{2}\bar{1}\}$ p-n structures, the built-in field and polarisation induced field are subtractive, resulting in a more rectangular and thus desirable QW potential profile compared to $\{20\bar{2}1\}$ QW structures. $\{20\bar{2}\bar{1}\}$ plane multiple QW LED structures have also been shown to exhibit improved hole transport relative to $\{20\bar{2}1\}$ plane MQW LEDs.⁹⁵ It has also been reported that the $\{20\bar{2}\bar{1}\}$ plane exhibits a higher optical polarisation ratio relative to the $\{20\bar{2}1\}$ plane.⁹⁶

There have been several reports of $\{20\bar{2}\bar{1}\}$ LEDs grown cut substrates with favourable performance in the green (~ 515 nm) and yellow green spectral range (~ 550 nm).^{97–99} It has been suggested that the more uniform indium incorporation along these planes for InGaN QW growth results in low spectral blue shift with increasing injection (due to localisation related effects) and a narrow spectral linewidth relative to other growth planes, both desirable properties for LEDs.

The EQEs reported in Ref. 97, 20% at 516 nm and 12.6% at 552 nm for drive currents of 20 mA, compare

very well with efficiencies reported in the literature for c plane devices emitting at similar wavelengths where sub-10% EQEs have been reported although no corresponding drive current has been given for these EQEs.^{100,101} While it is important to note that it is very difficult to directly compare EQE values given without a corresponding drive current and that EQE can be dependent on light extraction from the LED and other factors outside the internal quantum efficiency, the given values for semipolar LEDs emitting in the green and green yellow spectral ranges seem very encouraging.

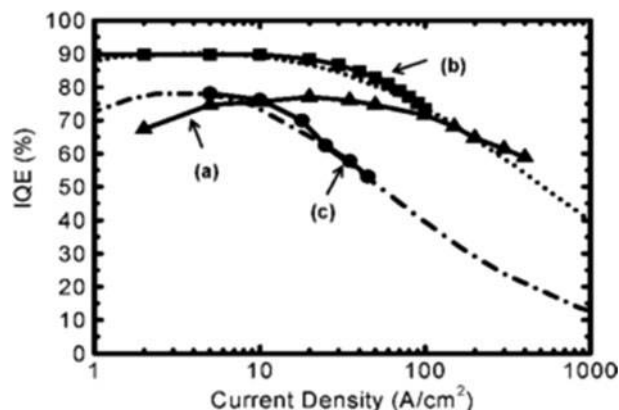
Semipolar LEDs may be useful for operation in the blue spectral range where c plane devices exhibit extremely high EQEs ($\sim 84\%$)⁷⁵ but also severe efficiency droop.⁴⁴ The ability to grow larger QWs relative to polar LEDs allows for the reduction in carrier density and thus efficiency droop and has been reported to consequently allow for reduced droop at high drive currents¹⁰² as shown in Fig. 18, as well as a reduction in thermal droop.¹⁰³ One could thus foresee an application for semipolar LEDs in high brightness low area LED applications.⁷⁴

Despite these promising results, issues inherent to the heteroepitaxial growth remain in the implementation of semipolar LED devices. The prohibitive price of bulk GaN substrate cutting remains a key issue to be overcome before semipolar and non-polar LEDs can compete commercially with current c plane LEDs in terms of production costs.

Doping

The intentional incorporation of impurities in III-nitrides has been reported to provide beneficial control of the QCSE. It has been suggested that this is achieved through several mechanisms that shall be discussed in this section.

There is a wealth of evidence suggesting that doping the QBs increases oscillator strength and reduces band-gap narrowing through free carrier screening of the QCSE.^{105–107} Di Carlo *et al.* used self-consistent tight binding calculations to demonstrate a blue shift in the optical transition energy for highly doped barriers in AlGaIn–GaIn QWs that was more prominent at lower



18 Comparison of internal quantum efficiency for a $\{20\bar{2}1\}$ (Ref. 102), b c plane,⁷⁵ and c c plane;¹⁰⁴ all devices emit at ~ 450 nm (blue); although c plane devices exhibit higher efficiencies at lower current densities, reduction of efficiency droop allows semipolar LED to exhibit higher efficiencies at large current densities⁴⁶

injected carrier density, consistent with the idea of dopant screening rather than injected carrier screening.¹⁰⁶ Choi *et al.* studied a series of InGaN/GaN QW structures with various doping levels to determine that the piezoelectric fields in the QWs were screened from Si donors in the barriers due to a reduction in Stokes shift with increasing doping level.¹⁰⁵ Esmaeili *et al.* reported the effect of doping on AlGaIn/GaN QW structures by establishing that the screening effect of photogenerated carriers in their PL study was minimal in moderately and heavily doped samples, indicating that the carriers originating from the doped barriers dominated the screening effect in these samples rather than injected carriers.¹⁰⁷

Some reports indicate that carrier localisation through QW width fluctuations or indium content fluctuations is also responsible for the perceived blue shift in PL. It has been suggested that the introduction of silicon doping can cause the InGaN QWs in some structures to undergo strain relaxation by decomposing,^{108,109} thus creating localisation centres and enhancing radiative efficiency. However, it is important to note that these results implying the generation of high indium content clusters were obtained by strain state analysis of TEM images, a technique O'Neil *et al.* and Smeeton *et al.* showed to be particularly susceptible to false detection due to strain induced by the imaging method itself,^{110,111} and indeed, it has been suggested that the optical properties of InGaN QWs may be influenced by ordering rather than clustering.¹¹² Furthermore, it has been shown that localisation of carriers can be induced by random indium alloy fluctuations as well as monolayer QW thickness fluctuations in undoped QW structures without the presence of gross indium clusters,¹¹³ thus casting some doubt over claims that silicon doping can induce indium clustering and be responsible for higher radiative efficiency.

Despite the numerous PL studies that indicate that doping can help alleviate symptoms of the QCSE, it is also important to consider the effect this can have on the electrical properties of an LED. The excessive silicon doping of QBs can, in fact, exert a 'hole blocking effect' on the whole structure, hindering the transport of positive carriers throughout the structure,¹¹⁴ which can result in a significant decrease in EL intensity.¹¹⁵

Strain control

The piezoelectric component tends to dominate the internal fields for (0001) InGaN/GaN QWs, and as such, an effective method of reducing the deleterious effects of the QCSE in these structures is to control the strain in the QW layer by manipulating the strain states of adjacent layers.³⁰

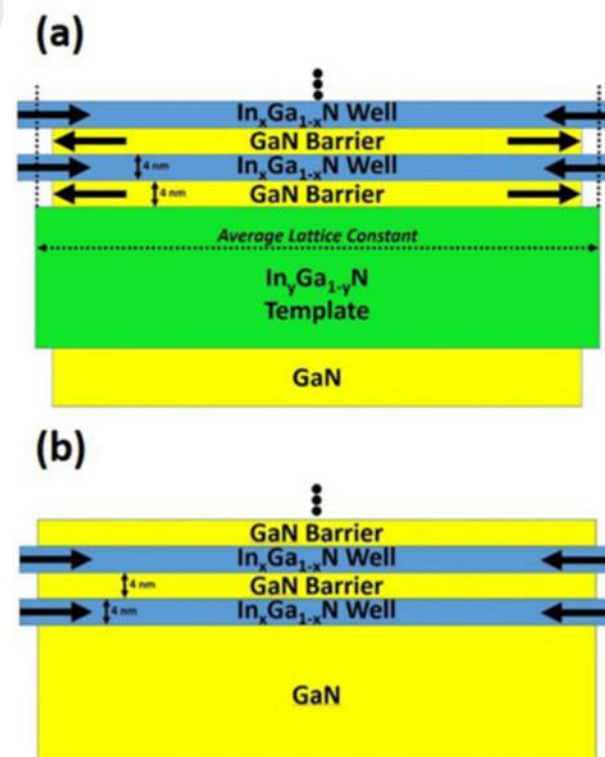
Nanhui *et al.* investigated the effect of strain relaxation on the optoelectronic properties of InGaN/GaN QW structures through the growth of InGaIn underlayers intended to act as strain relief layers.¹¹⁶ The authors reported a twofold increase in PL intensity for the structure with the underlayer relative to the control structure and a blue shift in peak emission wavelength, attributed to the partial relaxation of strain in the QW layer. Furthermore, the density of V pits, whose formation is commonly attributed to strain relaxation, was reduced from $16\text{--}18 \times 10^8$ to $6\text{--}7 \times 10^8 \text{ cm}^{-2}$. A further study by the authors revealed a decrease in the

maximum blue shift between low and high current densities for the strain relaxed samples grown on InGaIn/GaN superlattices relative to the standard QW structure.¹¹⁷

While the addition of an underlayer can help manage strain, it is also possible to change the layers grown above the active region to engineer strain. Ryou *et al.* reported a reduced blue shift with increasing injection current in a structure with a p-InGaIn layer relative to a structure with a p-GaN layer.²¹ The authors also reported considerably higher peak EL intensity for the p-InGaIn structure. Both the reduced blue shift and the increased EL intensity were attributed to the reduction of compressive strain on the InGaIn QW by employing a p layer with lower lattice mismatch to the QWs.

More recently, van den Broeck *et al.* reported strain balancing through the use of a thick $\text{In}_y\text{Ga}_{1-y}\text{N}$ template for the growth of $\text{In}_x\text{Ga}_{1-x}\text{N}/\text{GaN}$ QWs, where $x > y$.¹¹⁸ The template used was grown far beyond the critical layer thickness to ensure full relaxation. As such, the active region of QWs grown on this relaxed layer was strained to the lattice constant of the template rather than of the GaN substrate, as shown in Fig. 19.

This approach leads to compressive strain on the InGaIn wells and tensile strain for the GaN barriers. By optimising the indium content of the QWs and the strain balancing template, the authors reported fully strain balanced structures, with no strain relaxation effects observed for increasing number of QWs grown on the balanced templates. Furthermore, the strain balanced structures exhibited higher emission intensity, indicative of a reduction in the strain induced piezoelectric field.



19 **a** Strain balanced InGaIn/GaN structure grown on lower indium content InGaIn template and **b** conventional QW structure on GaN¹¹⁸

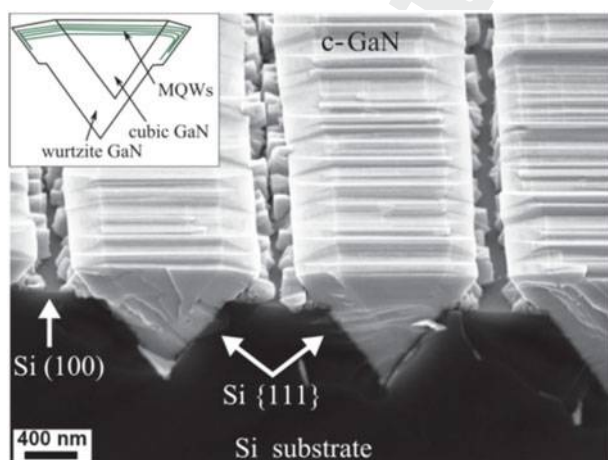
It is also important to note the effect of strain on indium incorporation for III-nitride structures when considering strain as a method of controlling the QCSE. Pereira *et al.* used depth resolved cathodoluminescence, Rutherford backscattering spectrometry¹¹⁹ and X-ray reciprocal space mapping¹²⁰ to demonstrate that the strain can obstruct the incorporation of indium atoms in an InGaN lattice. As such, the design of devices emitting at longer wavelengths requires careful consideration if strain relaxation techniques are used to control the QCSE as the interplay between strain, indium incorporation and emission wavelength must be taken into account.

Cubic III-nitrides

Zinc blende (cubic) III-nitrides offer an alternative way of eliminating polarisation fields inherent to their wurtzite counterparts. Recently, interest in cubic III-nitride growth can be attributed to several factors: cleaving (001) oriented zinc blende GaN along the vertical $\{110\}$ plane,¹²¹ enhanced p type carrier mobility¹²² and of course the removal of polarisation fields. Cubic InGaN/GaN QW structures are also expected to have the additional advantage of an inherently lower bandgap, thus requiring a lower indium composition for long wavelength devices.¹²³

Cubic III-nitride growth has been demonstrated on (0 0 1) GaAs,¹²⁴ (0 0 1) Si,¹²⁵ sapphire and (1 1 1) GaAs. Li *et al.* demonstrated room temperature green light emission from LED cubic InGaN/GaN QWs grown on 3C-SiC substrates and reported increasing PL intensity for larger well widths, indicating the absence of polarisation fields.¹²⁶ More recently, Stark *et al.* demonstrated EL from cubic InGaN/GaN LED structures grown on structured V grooves in Si (1 0 0) substrates and reported injection current independent emission wavelength, with few line defects or wurtzite inclusions within the cubic GaN.¹²⁷ Despite this, the difficulty of growing cubic GaN can be seen from the rough and discontinuous surface shown in Fig. 20.

While the development of cubic GaN does have many potential advantages for LED structures, the necessity for additional processing steps due to the higher



20 Scanning electron microscopy image of cross-section of cubic InGaN/GaN QWs grown on patterned Si (1 0 0) substrate; 'V' shaped boundary between wurtzite and cubic GaN can be seen from image contrast¹²⁷

thermodynamic stability of wurtzite GaN and the lack of material yield and quality renders this method of mitigating polarisation fields less attractive from an industrial and commercial point of view.

Conclusions

III-Nitride LEDs have already revolutionised the lighting industry, allowing for unprecedented energy savings on a global scale. However, in order to further improve their performance, the impact of the polarisation fields inherent to these materials must be controlled. This review has outlined the deleterious effects of polarisation fields on the emission properties of III-nitride QWs and several methods of controlling these detrimental effects.

In many cases, advances in device development have been swift, but a full understanding of the unique material challenges in controlling the polarisation fields for LEDs has been slower to materialise. Particularly in the case of alternative growth planes, considered the most promising method of mitigating the QCSE, the reduction of BSFs and high quality heteroepitaxial growth remain a priority and are the main obstacles preventing non-/semipolar LEDs from being commercially viable.

At present, it seems that semipolar growth for the mitigation of polarisation fields seems to be the most successful approach, particularly for long wavelength LEDs. These have demonstrated high efficiencies and low efficiency droop, although the efficiencies demonstrated in the blue spectral wavelength still lag behind those of *c* plane LEDs at lower injection currents. However, there is a distinct lack of comparison between efficiencies reported in the literature for LEDs grown on alternative growth planes, using strain or doping engineering, and normal *c* plane. A consistent method of comparison, whether it be for the same target emission wavelength, indium compositions or drive current, is required in order to truly assess the success of polarisation field mitigation techniques.

The strong impact III-nitride LED research continues to have commercially and industrially is perhaps best highlighted by this: although high performance devices may be achieved using various methods discussed throughout this review, a key consideration remains the feasibility of commercialisation, without which the development of a device cannot be considered a complete success.

References

1. 'The Nobel Prize in Physics', *Nobel Media*, 2014, http://www.nobelprize.org/nobel_prizes/physics/laureates/2014/ (accessed 20 February 2015).
2. McKinsey: 'Lighting the way: perspectives on the global lighting market'.
3. S. Nakamura, T. Mukai and M. Senoh: 'High-power GaN p-n junction blue-light-emitting diodes', *Jpn J. Appl. Phys.*, 1991, **30**, (12A), 1998–2001.
4. F. Scholz: 'Semipolar GaN grown on foreign substrates: a review', *Semicond. Sci. Technol.*, 2012, **27**, (2), 024002.
5. S. E. Bennett: 'Dislocations and their reduction in GaN', *Mater. Sci. Technol.*, 2010, **26**, (9), 1017–1028.
6. R. Oliver: 'Growth and characterisation of nitride nanostructures', *Mater. Sci. Technol.*, 2002, **18**, 1257–1271.
7. F. Bernardini, V. Fiorentini and D. Vanderbilt: 'Spontaneous polarization and piezoelectric constants of III-V nitrides', *Phys. Rev. B*, 1997, **56B**, (16), R10024–R10027.

8. K. Montgomery: 'kylemontgomery.net', 2014, <http://www.kmontgomery.net/> (accessed 5 February 2015).
9. O. Ambacher: 'Growth and applications of group III-nitrides', *J. Phys. D*, 1999, **31D**, 2653–2710.
10. O. Ambacher and J. Majewski: 'Pyroelectric properties of Al (In) GaN/GaN hetero- and quantum well structures', *J. Phys. Condens. Matter*, 2002, **3399**.
11. J. Lähnemann, O. Brandt, U. Jahn, C. Pfüller, C. Roder, P. Dogan, F. Grosse, A. Belabbes, F. Bechstedt, A. Trampert and L. Geelhaar: 'Direct experimental determination of the spontaneous polarization of GaN', *Phys. Rev. B*, 2012, **86B**, 1–5.
12. E. T. Yu, X. Z. Dang, P. M. Asbeck, S. S. Lau and G. J. Sullivan: 'Spontaneous and piezoelectric polarization effects in III–V nitride heterostructures', *J. Vac. Sci. Technol. B*, 1999, **17B**, 1742.
13. C. Wood and D. Jena: 'Polarization effects in semiconductors: from ab initio theory to device applications', 2007, Springer.
14. P. Waltereit, O. Brandt, A. Trampert, H. Grahn, J. Menniger, M. Ramsteiner, M. Reiche and K. Ploog: 'Nitride semiconductors free of electrostatic fields for efficient white light-emitting diodes', *Nature*, 2000, **406**, (6798), 865–868.
15. K. S. Ramaiah, Y. K. Su, S. J. Chang, B. Kerr, H. P. Liu and I. G. Chen: 'Characterization of InGaN/GaN multi-quantum-well blue-light-emitting diodes grown by metal organic chemical vapor deposition', *Appl. Phys. Lett.*, 2004, **84**, (17), 3307–3309.
16. M. J. Galtrey, R. A. Oliver, M. J. Kappers, C. J. Humphreys, P. H. Clifton, D. Larson, D. W. Saxey and A. Cerezo: 'Three-dimensional atom probe analysis of green- and blue-emitting In_xGa_{1-x}N/GaN multiple quantum well structures', *J. Appl. Phys.*, 2008, **104**, (1), 013524.
17. H. Amari, I. M. Ross, T. Wang and T. Walther: 'Characterization of InGaN/GaN epitaxial layers by aberration corrected TEM/STEM', *Phys. Status Solidi C*, 2012, **9C**, (3–4), 546–549.
18. T. Walther, H. Amari, I. M. Ross, T. Wang and A. G. Cullis: 'Lattice resolved annular dark-field scanning transmission electron microscopy of (Al, In)GaN/GaN layers for measuring segregation with sub-monolayer precision', *J. Mater. Sci.*, 2013, **48**, (7), 2883–2892.
19. F. C. -P. Massabuau, M. J. Davies, W. E. Blenkhorn, S. Hammersley, M. J. Kappers, C. J. Humphreys, P. Dawson and R. A. Oliver: 'Investigation of unintentional indium incorporation into GaN barriers of InGaN/GaN quantum well structures', *Phys. Status Solidi*, 2014.
20. D. A. B. Miller, D. S. Chemla, T. C. Damen, A. C. Gossard, W. Wiegmann, T. H. Wood and C. A. Burrus: 'Band-edge electroabsorption in quantum well structures: the quantum-confined stark effect', *Phys. Rev. Lett.*, 1984, **53**, (22), 2173–2176.
21. J. -H. Ryou, W. Lee, J. Limb, D. Yoo, J. P. Liu, R. D. Dupuis, Z. H. Wu, A. M. Fischer and F. A. Ponce: 'Control of quantum-confined Stark effect in InGaN/GaN multiple quantum well active region by p-type layer for III-nitride-based visible light emitting diodes', *Appl. Phys. Lett.*, 2008, **92**, (10), 101113.
22. V. Fiorentini, F. Bernardini, F. Della Sala, A. Di Carlo, P. Lugli and T. Vergata: 'Effects of macroscopic polarization in III–V nitride multiple quantum wells', *Phys. Rev. B*, 1999, **60B**, (12), 8849–8858.
23. S. F. Chichibu, A. Uedono, T. Onuma, B. A. Haskell, A. Chakraborty, T. Koyama, P. T. Fini, S. Keller, S. P. Denbaars, J. S. Speck, U. K. Mishra, S. Nakamura, S. Yamaguchi, S. Kamiyama, H. Amano, I. Akasaki, J. Han and T. Sota: 'Origin of defect-insensitive emission probability in In-containing (Al, In, Ga)N alloy semiconductors', *Nat. Mater.*, 2006, **5**, (10), 810–816.
24. D. Cherns, J. Barnard and F. A. Ponce: 'Measurement of the piezoelectric field across strained InGaN/GaN layers by electron holography', *Solid State Commun.*, 1999, **111**, (5), 281–285.
25. M. Stevens, A. Bell, M. R. McCartney, F. A. Ponce, H. Marui and S. Tanaka: 'Effect of layer thickness on the electrostatic potential in InGaN quantum wells', *Appl. Phys. Lett.*, 2004, **85**, (20), 4651–4653.
26. M. R. McCartney, F. A. Ponce, J. Cai and D. P. Bour: 'Mapping electrostatic potential across an AlGaIn/InGaIn/AlGaIn diode by electron holography', *Appl. Phys. Lett.*, 2000, **76**, (21), 3055.
27. D. Cherns and C. Jiao: 'Electron holography studies of the charge on dislocations GaN', *Phys. Rev. Lett.*, 2001, **87**, (20), 205504.
28. J. Cai and F. A. Ponce: 'Determination by electron holography of the electronic charge distribution at threading dislocations in epitaxial GaN', *Phys. Status Solidi Appl. Res.*, 2002, **192**, (2), 407–411.
29. T. Takeuchi, S. Sota, M. Katsuragawa, M. Komori, H. Takeuchi, H. Amano and I. Akasaki: 'Quantum-confined stark effect due to piezoelectric fields in GaInN strained quantum wells', *Jpn J. Appl. Phys.*, 1997, **36**, L382–L385.
30. J. H. Ryou, P. D. Yoder, J. Liu, Z. Lochner, H. S. Kim, S. Choi, H. J. Kim and R. D. Dupuis: 'Control of quantum-confined stark effect in InGaIn-based quantum wells', *IEEE J. Sel. Top. Quantum Electron.*, 2009, **15**, (4), 1080–1091.
31. H. S. Kim, J. Y. Lin, H. X. Jiang, W. W. Chow, A. Botchkarev and H. Morkoç: 'Piezoelectric effects on the optical properties of GaN/Al_xGa_{1-x}N multiple quantum wells', *Appl. Phys. Lett.*, 1998, **73**, (1998), 3426–3428.
32. T. Takeuchi, C. Wetzel, S. Yamaguchi, H. Sakai, H. Amano, I. Akasaki, Y. Kaneko, S. Nakagawa, Y. Yamaoka and N. Yamada: 'Determination of piezoelectric fields in strained GaInN quantum wells using the quantum-confined Stark effect', *Appl. Phys. Lett.*, 1998, **73**, (1998), 1691–1693.
33. H. Obloh, K. Bachem, U. Kaufmann, M. Kunzer, M. Maier, A. Ramakrishnan and P. Schlotter: 'Self-compensation in Mg doped p-type GaN grown by MOCVD', *J. Cryst. Growth*, 1998, **195**, (1–4), 270–273.
34. B. S. Simpkins: 'Local conductivity and surface photovoltage variations due to magnesium segregation in p-type GaN', *J. Appl. Phys.*, 2004, **95**, (11), 6225.
35. S. E. Bennett, R. M. Ulfig, P. H. Clifton, M. J. Kappers, J. S. Barnard, C. J. Humphreys and R. A. Oliver: 'Atom probe tomography and transmission electron microscopy of a Mg-doped AlGaIn/GaN superlattice', *Ultramicroscopy*, 2011, **111**, (3), 207–211.
36. L. S. Wang, W. K. Fong, C. Surya, K. W. Cheah, W. H. Zheng and Z. G. Wang: 'Photoluminescence of rapid-thermal annealed Mg-doped GaN films', *Solid State Electron.*, 2001, **45**, 1153–1157.
37. Z. G. Ju, S. T. Tan, Z. -H. Zhang, Y. Ji, Z. Kyaw, Y. Dikme, X. W. Sun and H. V. Demir: 'On the origin of the redshift in the emission wavelength of InGaIn/GaN blue light emitting diodes grown with a higher temperature interlayer', *Appl. Phys. Lett.*, 2012, **100**, (12), 123503.
38. A. Jarjour, R. Oliver, A. Tahraoui, M. Kappers, C. Humphreys and R. Taylor: 'Control of the oscillator strength of the exciton in a single InGaIn–GaN quantum dot', *Phys. Rev. Lett.*, 2007, **99**, (19), 197403.
39. P. Hannaford: 'The oscillator strength in atomic absorption spectroscopy', *Microchem. J.*, 1999, **63**, 43–52.
40. J. Seo Im, H. Kollmer, J. Off, A. Sohmer, F. Scholz and A. Hangleiter: 'Reduction of oscillator strength due to piezoelectric fields in GaN/Al_xGa_{1-x}N quantum wells', *Phys. Rev. B*, 1998, **57B**, (16), R9435–R9438.
41. S. Chichibu, A. Abare, M. Mack, M. Minsky, T. Deguchi, D. Cohen, P. Kozodoy, S. Fleischer, S. Keller, J. Speck, J. Bowers, E. Hu, U. Mishra, L. Coldren, S. DenBaars, K. Wada, T. Sota and S. Nakamura: 'Optical properties of InGaIn quantum wells', *Mater. Sci. Eng. B*, 1999, **B59**, (1–3), 298–306.
42. N. Grandjean, B. Damilano and J. Massies: 'Group-III nitride quantum heterostructures grown by molecular beam epitaxy', *J. Phys. Condens. Matter*, 2001, **13**, 6945–6960.
43. N. Shmidt, A. Greshnov, A. Chernyakov, M. Levinshstein, A. Zakgeim and E. Shabunina: 'Mechanisms behind efficiency droop and degradation in InGaIn/GaN LEDs', *Phys. Status Solidi*, 2013, **10**, (3), 332–334.
44. M. -H. Kim, M. F. Schubert, Q. Dai, J. K. Kim, E. F. Schubert, J. Piprek and Y. Park: 'Origin of efficiency droop in GaN-based light-emitting diodes', *Appl. Phys. Lett.*, 2007, **91**, (18), 183507.
45. Z. Zheng, Z. Chen, Y. Chen, H. Wu, S. Huang and B. Fan: 'Improved carrier injection and efficiency droop in InGaIn/GaN light-emitting diodes with step-stage multiple-quantum-well structure and hole-blocking barriers', 2013, **241108**, (2013).
46. S. Nakamura and M. R. Krames: 'History of gallium-nitride-based light-emitting diodes for illumination', *Proc. IEEE*, 2013, **101**, (10), 2211–2220.
47. T. Takeuchi, H. Amano and I. Akasaki: 'Theoretical study of orientation dependence of piezoelectric effects in wurtzite strained GaInN/GaN heterostructures and quantum wells', *Jpn J. Appl. Phys.*, 2000, **39**, (Part 1), 413–416.
48. S. Schwaiger, S. Metzner, T. Wunderer, I. Argut, J. Thalmer, F. Lipski, M. Wieneke, J. Bläsing, F. Bertram, J. Zweck, A. Krost, J. Christen and F. Scholz: 'Growth and coalescence behavior of semipolar [1122] GaN on pre-structured r-plane sapphire substrates', *Phys. Status Solidi*, 2011, **248**, (3), 588–593.
49. R. M. Farrell, E. C. Young, F. Wu, S. P. DenBaars and J. S. Speck: 'Materials and growth issues for high-performance

- nonpolar and semipolar light-emitting devices', *Semicond. Sci. Technol.*, 2012, **27**, 024001.
50. P. Gibart: 'Metal organic vapour phase epitaxy of GaN and lateral overgrowth', *Rep. Prog. Phys.*, 2004, **67**, (5), 667–715.
 51. T. Wang, J. Bai, S. Sakai and J. K. Ho: 'Investigation of the emission mechanism in InGaN/GaN-based light-emitting diodes', *Appl. Phys. Lett.*, 2001, **78**, (2001), 2617–2619.
 52. J. Bai, T. Wang and S. Sakai: 'Influence of the quantum-well thickness on the radiative recombination of InGaN/GaN quantum well structures', *J. Appl. Phys.*, 2000, **88**, (2000), 4729.
 53. T. W. Weeks, M. D. Bremser, K. S. Ailey, E. Carlson, W. G. Perry, E. L. Piner, N. A. El-Masry and R. F. Davis: 'Undoped and doped GaN thin films deposited on high-temperature monocrystalline AlN buffer layers on vicinal and on-axis α (6H)-SiC(0001) substrates via organometallic vapor phase epitaxy', *J. Mater. Res.*, 1996, **11**, (04), 1011–1018.
 54. E. Valcheva, T. Paskova, S. Tungasmita, P. O. Å. Persson, J. Birch, E. B. Svedberg, L. Hultman and B. Monemar: 'Interface structure of hydride vapor phase epitaxial GaN grown with high-temperature reactively sputtered AlN buffer', *Appl. Phys. Lett.*, 2000, **76**, (14), 1860–1862.
 55. F. Oehler, D. Sutherland, T. Zhu, R. Emery, T. J. Badcock, M. J. Kappers, C. J. Humphreys, P. Dawson and R. A. Oliver: 'Evaluation of growth methods for the heteroepitaxy of non-polar (11 $\bar{2}$ 0) GaN on sapphire by MOVPE', *J. Cryst. Growth*, 2014, **408**, 32–41.
 56. B. M. Imer, F. Wu, S. P. Denbaars and J. S. Speck: 'Improved quality (11 $\bar{2}$ 0) *a*-plane GaN with sidewall lateral epitaxial overgrowth', *Appl. Phys. Lett.*, 2006, **88**, (2006), 86–89.
 57. A. Chitnis, C. Chen, V. Adivarahan, M. Shatalov, E. Kuokstis, V. Mandavilli, J. Yang and M. A. Khan: 'Visible light-emitting diodes using *a*-plane GaN-InGaN multiple quantum wells over *r*-plane sapphire', *Appl. Phys. Lett.*, 2004, **84**, (18), 3663.
 58. A. Chakraborty, B. A. Haskell, S. Keller, J. S. Speck, S. P. DenBaars, S. Nakamura and U. K. Mishra: 'Nonpolar InGaN/GaN emitters on reduced-defect lateral epitaxially overgrown *a*-plane GaN with drive-current-independent electroluminescence emission peak', *Appl. Phys. Lett.*, 2004, **85**, (22), 5143.
 59. A. Chakraborty, S. Keller, C. Meier, B. A. Haskell, S. Keller, P. Waltereit, S. P. DenBaars, S. Nakamura, J. S. Speck and U. K. Mishra: 'Properties of nonpolar *a*-plane InGaN/GaN multiple quantum wells grown on lateral epitaxially overgrown *a*-plane GaN', *Appl. Phys. Lett.*, 2005, **86**, (3), 031901.
 60. K. J. Fujian, M. Feneberg, B. Neuschl, T. Meisch, I. Tischer, K. Thonke, S. Schwaiger, I. Izadi, F. Scholz, L. Lechner, J. Biskupek and U. Kaiser: 'Cathodoluminescence of GaInN quantum wells grown on nonpolar *a* plane GaN: intense emission from pit facets', *Appl. Phys. Lett.*, 2010, **97**, (2010), 1–4.
 61. C. Mauder, B. Reuters, L. Rahimzadeh Khoshroo, M. V. Rzheutskii, E. V. Lutsenko, G. P. Yablonskii, J. F. Woitok, M. Heuken, H. Kalisch and R. H. Jansen: 'Development of *m*-plane GaN anisotropic film properties during MOVPE growth on LiAlO₂ substrates', *J. Cryst. Growth*, 2010, **312**, (11), 1823–1827.
 62. B. Liu, R. Zhang, Z. L. Xie, C. X. Liu, J. Y. Kong, J. Yao, Q. J. Liu, Z. Zhang, D. Y. Fu, X. Q. Xiu, H. Lu, P. Chen, P. Han, S. L. Gu, Y. Shi, Y. D. Zheng, J. Zhou and S. M. Zhou: 'Nonpolar *m*-plane thin film GaN, InGaN/GaN light-emitting diodes on LiAlO₂(100) substrates', *Appl. Phys. Lett.*, 2007, **91**, (25), 253506.
 63. Y. S. Cho, Q. Sun, I. -H. Lee, T. -S. Ko, C. D. Yerino, J. Han, B. H. Kong, H. K. Cho and S. Wang: 'Reduction of stacking fault density in *m*-plane GaN grown on SiC', *Appl. Phys. Lett.*, 2008, **93**, (11), 111904.
 64. K. C. Kim, M. C. Schmidt, F. Wu, M. B. McLaurin, A. Hirai, S. Nakamura, S. P. Denbaars and J. S. Speck: 'Low extended defect density nonpolar *m*-plane GaN by sidewall lateral epitaxial overgrowth', *Appl. Phys. Lett.*, 2008, **93**, (2008), 2006–2009.
 65. B. A. Haskell, F. Wu, M. D. Craven, S. Matsuda, P. T. Fini, T. Fujii, K. Fujito, S. P. DenBaars, J. S. Speck and S. Nakamura: 'Defect reduction in (11 $\bar{2}$ 0) *a*-plane gallium nitride via lateral epitaxial overgrowth by hydride vapor-phase epitaxy', *Appl. Phys. Lett.*, 2003, **83**, (2003), 644–646.
 66. B. A. Haskell, T. J. Baker, M. B. McLaurin, F. Wu, P. T. Fini, S. P. Denbaars, J. S. Speck and S. Nakamura: 'Defect reduction in (1 $\bar{1}$ 00) *m*-plane gallium nitride via lateral epitaxial overgrowth by hydride vapor phase epitaxy', *Appl. Phys. Lett.*, 2005, **86**, (2005), 1–3.
 67. K. Okamoto, H. Ohta, D. Nakagawa, M. Sonobe, J. Ichihara and H. Takasu: 'Dislocation-free *m*-plane InGaN/GaN light-emitting diodes on *m*-plane GaN single crystals', *Jpn J. Appl. Phys.*, 2006, **45**, L1197–L1199.
 68. M. C. Schmidt, K. C. Kim, H. Sato, N. Fellows, H. Masui, S. Nakamura, S. P. DenBaars and J. S. Speck: 'High power and high external efficiency *m*-plane InGaN light emitting diodes', *Jpn J. Appl. Phys.*, 2007, **46**, (Part 2), 7–10.
 69. T. Detchprohm, M. Zhu, Y. Li, L. Zhao, S. You, C. Wetzel, E. A. Preble, T. Paskova and D. Hanser: 'Wavelength-stable cyan and green light emitting diodes on nonpolar *m*-plane GaN bulk substrates', *Appl. Phys. Lett.*, 2010, **96**, (2010), 10–13.
 70. F. Wu, Y. Lin, A. Chakraborty, H. Ohta, S. P. DenBaars, S. Nakamura and J. S. Speck: 'Stacking fault formation in the long wavelength InGaN/GaN multiple quantum wells grown on *m*-plane GaN', *Appl. Phys. Lett.*, 2010, **96**, (2010), 231912.
 71. Y. Da Lin, A. Chakraborty, S. Brinkley, H. C. Kuo, T. Melo, K. Fujito, J. S. Speck, S. P. Denbaars and S. Nakamura: 'Characterization of blue-green *m*-plane InGaN light emitting diodes', *Appl. Phys. Lett.*, 2009, **94**, (2009), 10–13.
 72. K. C. Kim, M. C. Schmidt, H. Sato, F. Wu, N. Fellows, M. Saito, K. Fujito, J. S. Speck, S. Nakamura and S. P. DenBaars: 'Improved electroluminescence on nonpolar *m*-plane InGaN/GaN quantum wells LEDs', *Phys. Status Solidi RRL*, 2007, **1**, (3), 125–127.
 73. A. Chakraborty, B. A. Haskell, S. Keller, J. S. Speck, S. P. Denbaars, S. Nakamura and U. K. Mishra: 'Demonstration of nonpolar *m*-plane InGaN/GaN light-emitting diodes on free-standing *m*-plane GaN substrates', *Jpn J. Appl. Phys.*, 2005, **44**, L173–L175.
 74. S. P. Denbaars, D. Feezell, K. Kelchner, S. Pimpitkar, C. C. Pan, C. C. Yen, S. Tanaka, Y. Zhao, N. Pfaff, R. Farrell, M. Iza, S. Keller, U. Mishra, J. S. Speck and S. Nakamura: 'Development of gallium-nitride-based light-emitting diodes (LEDs) and laser diodes for energy-efficient lighting and displays', *Acta Mater.*, 2013, **61**, (3), 945–951.
 75. Y. Narukawa, M. Ichikawa, D. Sanga, M. Sano and T. Mukai: 'White light emitting diodes with super-high luminous efficacy', *J. Phys. D*, 2010, **43D**, 354002.
 76. S. C. Ling, T. C. Lu, S. P. Chang, J. R. Chen, H. C. Kuo and S. C. Wang: 'Low efficiency droop in blue-green *m*-plane InGaN/GaN light emitting diodes', *Appl. Phys. Lett.*, 2010, **96**, (2010), 2008–2011.
 77. A. E. Romanov, T. J. Baker, S. Nakamura and J. S. Speck: 'Strain-induced polarization in wurtzite III-nitride semipolar layers', *J. Appl. Phys.*, 2006, **100**, (2), 023522.
 78. T. Matsuoka and E. Hagiwara: 'GaN growth on novel lattice-matching substrate: tilted *m*-plane sapphire', *Phys. Status Solidi A*, 2001, **188A**, (2), 485–489.
 79. Q. Sun, B. Leung, C. D. Yerino, Y. Zhang and J. Han: 'Improving microstructural quality of semipolar (11 $\bar{2}$ 2) GaN on *m*-plane sapphire by a two-step growth process', *Appl. Phys. Lett.*, 2009, **95**, 0–3.
 80. T. Wernicke, C. Netzel, M. Weyers and M. Kneissl: 'Semipolar GaN grown on *m*-plane sapphire using MOVPE', *Phys. Status Solidi C*, 2008, **5C**, (6), 1815–1817.
 81. C. F. Johnston, M. J. Kappers, M. A. Moram, J. L. Hollander and C. J. Humphreys: 'Defect reduction in non-polar (11 $\bar{2}$ 0) GaN grown on (1102) sapphire', *Phys. Status Solidi*, 2009, **206**, (6), 1190–1193.
 82. M. A. Moram, Y. Zhang, M. J. Kappers, Z. H. Barber and C. J. Humphreys: 'Dislocation reduction in gallium nitride films using scandium nitride interlayers', *Appl. Phys. Lett.*, 2007, **91**, (15), 152101.
 83. P. de Mierry, N. Kriouche, M. Nemoz and G. Nataf: 'Improved semipolar (11 $\bar{2}$ 2) GaN quality using asymmetric lateral epitaxy', *Appl. Phys. Lett.*, 2009, **94**, (19), 191903.
 84. S. Kamiyama, A. Honshio, T. Kitano, M. Iwaya, H. Amano, I. Akasaki, H. Kinoshita and H. Shiomi: 'GaN growth on (30 $\bar{3}$ 8) 4H-SiC substrate for reduction of internal polarization', *Phys. Status Solidi C*, 2005, **2C**, (7), 2121–2124.
 85. A. Chakraborty, T. J. Baker, B. A. Haskell, F. Wu, J. S. Speck, S. P. Denbaars, S. Nakamura and U. K. Mishra: 'Milliwatt power blue In GaN/GaN light-emitting diodes on semipolar GaN templates', *Jpn J. Appl. Phys.*, 2005, **44**, (Part 2), 7–10.
 86. M. Funato, M. Ueda, Y. Kawakami, Y. Narukawa, T. Kosugi, M. Takahashi and T. Mukai: 'Blue, green and amber In GaN/GaN light-emitting diodes on semipolar {11 $\bar{2}$ 2} GaN bulk substrates', *Jpn J. Appl. Phys.*, 2006, (Part 2), 45.

87. A. Tyagi, H. Zhong, N. N. Fellows, M. Iza, J. S. Speck, S. P. DenBaars and S. Nakamura: 'High brightness violet InGaN/GaN light emitting diodes on semipolar {10 $\bar{1}$ 1} bulk GaN substrates', *Jpn J. Appl. Phys.*, 2007, **46**, (Part 2), 10–13.
88. H. Zhong, A. Tyagi, N. N. Fellows, F. Wu, R. B. Chung, M. Saito, K. Fujito, J. S. Speck, S. P. DenBaars and S. Nakamura: 'High power and high efficiency blue light emitting diode on freestanding semipolar (10 $\bar{1}$ 1) bulk GaN substrate', *Appl. Phys. Lett.*, 2007, **90**, (2007), 233504.
89. Y. Zhao, J. Sonoda, C. C. Pan, S. Brinkley, I. Koslow, K. Fujito, H. Ohta, S. P. DenBaars and S. Nakamura: '30-mW-class high-power and high-efficiency blue semipolar (10 $\bar{1}$ 1) InGaN/GaN light-emitting diodes obtained by backside roughening technique', *Appl. Phys. Express*, 2010, **3**, (10), 10–13.
90. Y. Zhao, S. Tanaka, C. C. Pan, K. Fujito, D. Feezell, J. S. Speck, S. P. DenBaars and S. Nakamura: 'High-power blue-violet semipolar (20 $\bar{2}$ 1) InGaN/GaN light-emitting diodes with low efficiency droop at 200 A/cm²', *Appl. Phys. Express*, 2011, **4**, 2–5.
91. H. Sato, A. Tyagi, H. Zhong, N. N. Fellows, R. B. Chung, M. Saito, K. Fujito, J. S. Speck, S. P. DenBaars and S. Nakamura: 'High power and high efficiency green light emitting diode on free-standing semipolar {11 $\bar{2}$ 2} bulk GaN substrate', *Phys. Status Solidi RRL*, 2007, **1**, (4), 162–164.
92. H. Sato, R. B. Chung, H. Hirasawa, N. Fellows, H. Masui, F. Wu, M. Saito, K. Fujito, J. S. Speck, S. P. DenBaars and S. Nakamura: 'Optical properties of yellow light-emitting diodes grown on semipolar {11 $\bar{2}$ 2} bulk GaN substrates', *Appl. Phys. Lett.*, 2008, **92**, (2008), 221110.
93. J. E. Northrup: 'GaN and InGaN {11 $\bar{2}$ 2} surfaces: group-III adlayers and indium incorporation', *Appl. Phys. Lett.*, 2009, **95**, (2009), 10–13.
94. Y. Zhao, Q. Yan, C. Y. Huang, S. C. Huang, P. Shan Hsu, S. Tanaka, C. C. Pan, Y. Kawaguchi, K. Fujito, C. G. Van De Walle, J. S. Speck, S. P. DenBaars, S. Nakamura and D. Feezell: 'Indium incorporation and emission properties of nonpolar and semipolar InGaN quantum wells', *Appl. Phys. Lett.*, 2012, **100**, (20).
95. Y. Kawaguchi, C. Y. Huang, Y. R. Wu, Q. Yan, C. C. Pan, Y. Zhao, S. Tanaka, K. Fujito, D. Feezell, C. G. VanDe Walle, S. P. DenBaars and S. Nakamura: 'Influence of polarity on carrier transport in semipolar (20 $\bar{2}$ 1) and (20 $\bar{2}$ 1) multiple-quantum-well light-emitting diodes', *Appl. Phys. Lett.*, 2012, **100**, (23), 1–5.
96. Y. Zhao, S. Tanaka, Q. Yan, C. Y. Huang, R. B. Chung, C. C. Pan, K. Fujito, D. Feezell, C. G. Van De Walle, J. S. Speck, S. P. DenBaars and S. Nakamura: 'High optical polarization ratio from semipolar (20 $\bar{2}$ 1) blue-green InGaN/GaN light-emitting diodes', *Appl. Phys. Lett.*, 2011, **99**, (5), 97–100.
97. S. Yamamoto, Y. Zhao, C. C. Pan, R. B. Chung, K. Fujito, J. Sonoda, S. P. DenBaars and S. Nakamura: 'High-efficiency single-quantum-well green and yellow-green light-emitting diodes on semipolar (11 $\bar{2}$ 2) GaN substrates', *Appl. Phys. Express*, 2010, **3**.
98. R. B. Chung, Y. Da Lin, I. Koslow, N. Pfaff, H. Ohta, J. Ha, S. P. DenBaars and S. Nakamura: 'Electroluminescence characterization of (20 $\bar{2}$ 1) InGaN/GaN light emitting diodes with various wavelengths', *Jpn J. Appl. Phys.*, 2010, **49**, 0702031–0702033.
99. Y. Zhao, S. H. Oh, F. Wu, Y. Kawaguchi, S. Tanaka, K. Fujito, J. S. Speck, S. P. DenBaars and S. Nakamura: 'Green semipolar (20 $\bar{2}$ 1) InGaN light-emitting diodes with small wavelength shift and narrow spectral linewidth', *Appl. Phys. Express*, 2013, **6**.
100. M. Peter, A. Laubsch, P. Stauss, A. Walter, J. Baur and B. Hahn: 'Green ThinGaN power-LED demonstrates 100 lm', *Phys. Status Solidi C*, 2008, **5C**, (6), 2050–2052.
101. Osram: 'Osram achieves record figures with green LEDs', 2014, http://www.osram-os.com/osram_os/en/press/press-releases/led-for-automotive-consumer-industry/2014/osram-achieves-record-figures-with-green-leds/index.jsp (accessed 23 February 2015).
102. C. C. Pan, S. Tanaka, F. Wu, Y. Zhao, J. S. Speck, S. Nakamura, S. P. DenBaars and D. Feezell: 'High-power, low-efficiency-droop semipolar (20 $\bar{2}$ 1) single-quantum-well blue light-emitting diodes', *Appl. Phys. Express*, 2012, **5**.
103. C. C. Pan, T. Gilbert, N. Pfaff, S. Tanaka, Y. Zhao, D. Feezell, J. S. Speck, S. Nakamura and S. P. DenBaars: 'Reduction in thermal droop using thick single-quantum-well structure in semipolar (20 $\bar{2}$ 1) blue light-emitting diodes', *Appl. Phys. Express*, 2012, **5**, (10), 18–21.
104. K. J. Vampola, N. N. Fellows, H. Masui, S. E. Brinkley, M. Furukawa, R. B. Chung, H. Sato, J. Sonoda, H. Hirasawa, M. Iza, S. P. DenBaars and S. Nakamura: 'Highly efficient broad-area blue and white light-emitting diodes on bulk GaN substrates', *Phys. Status Solidi*, 2009, **206**, (2), 200–202.
105. C. Choi, Y. Kwon, B. Little, G. Gainer, J. Song, Y. Chang, S. Keller, U. Mishra and S. DenBaars: 'Time-resolved photoluminescence of In_xGa_{1-x}N/GaN multiple quantum well structures: effect of Si doping in the barriers', *Phys. Rev. B*, 2001, **64B**, 1–7.
106. A. Di Carlo, F. Della Sala, P. Lugli, V. Fiorentini and F. Bernardini: 'Doping screening of polarization fields in nitride heterostructures', *Appl. Phys. Lett.*, 2000, **76**, (2000), 3950–3952.
107. M. Esmaili, H. Haratizadeh and M. Gholami: 'Investigation of optical properties of modulation doped GaN/AlGaIn MQWS nanostructures', *Physica B*, 2009, **404B**, (21), 4233–4236.
108. M. Chen, Y. Cheng, J. Chen, C. Wu, C. C. Yang, K. Ma, J. Yang and A. Rosenauer: 'Effects of silicon doping on the nanostructures of InGaIn/GaN quantum wells', *J. Cryst. Growth*, 2005, **279**, 55–64.
109. Y. C. Cheng, E. C. Lin, C. M. Wu, C. C. Yang, J. R. Yang, A. Rosenauer, K. J. Ma, S. C. Shi, L. C. Chen, C. C. Pan and J. I. Chyi: 'Nanostructures and carrier localization behaviors of green-luminescence InGaIn/GaN quantum-well structures of various silicon-doping conditions', *Appl. Phys. Lett.*, 2004, **84**, (2004), 2506–2508.
110. J. P. O'Neill, I. M. Ross, A. G. Cullis, T. Wang and P. J. Parbrook: 'Electron-beam-induced segregation in InGaIn/GaN multiple-quantum wells', *Appl. Phys. Lett.*, 2003, **83**, (10), 1965–1967.
111. T. M. Smeeton, M. J. Kappers, J. S. Barnard, M. E. Vickers and C. J. Humphreys: 'Electron-beam-induced strain within InGaIn quantum wells: false indium "cluster" detection in the transmission electron microscope', *Appl. Phys. Lett.*, 2003, **83**, (26), 5419.
112. P. M. Albrecht, V. Grillo, J. Borysiuk, T. Remmele, H. P. Strunk, T. Walther, W. Mader, I. G., S. P. Prystawko and M. Leszczynski: 'Correlating compositional, structural and optical properties of InGaIn quantum wells by transmission electron microscopy', 'Proc. MSM-12, Oxford, UK', 85–88; 2001, .
113. D. Watson-Parris, M. J. Godfrey, P. Dawson, R. A. Oliver, M. J. Galtrey, M. J. Kappers and C. J. Humphreys: 'Carrier localization mechanisms in In_xGa_{1-x}N/GaN quantum wells', *Phys. Rev. B*, 2011, **83B**, (11), 115321.
114. E. H. Park, D. N. H. Kang, I. T. Ferguson, S. K. Jeon, J. S. Park and T. K. Yoo: 'The effect of silicon doping in the selected barrier on the electroluminescence of InGaIn/GaN multiquantum well light emitting diode', *Appl. Phys. Lett.*, 2007, **90**, (2007), 16–19.
115. J. H. Ryou, J. Limb, W. Lee, J. Liu, Z. Lochner, D. Yoo and R. D. Dupuis: 'Effect of silicon doping in the quantum-well barriers on the electrical and optical properties of visible green light-emitting diodes', *IEEE Photonics Technol. Lett.*, 2008, **20**, (21), 1769–1771.
116. N. Nanhui, W. Huaibing, L. Jianping, L. Naixin, X. Yanhui, H. Jun, D. Jun and S. Guangdi: 'Improved quality of InGaIn/GaN multiple quantum wells by a strain relief layer', *J. Cryst. Growth*, 2006, **286**, 209–212.
117. N. Nanhui, W. Huaibing, L. Jianping, L. Naixin, X. Yanhui, H. Jun, D. Jun and S. Guangdi: 'Enhanced luminescence of InGaIn/GaN multiple quantum wells by strain reduction', *Solid State Electron.*, 2007, **51**, 860–864.
118. D. M. Van Den Broeck, D. Bharrat, A. M. Hosalli, N. A. El-Masry and S. M. Bedair: 'Strain-balanced InGaIn/GaN multiple quantum wells', *Appl. Phys. Lett.*, 2014, **105**, 031107.
119. S. Pereira, M. R. Correia, E. Pereira, K. P. O'Donnell, C. Trager-Cowan, F. Sweeney and E. Alves: 'Compositional pulling effects in In_xGa_{1-x}N/GaN layers: a combined depth-resolved cathodoluminescence and Rutherford backscattering/channeling study', *Phys. Rev. B*, 2001, **64B**, 1–5.
120. S. Pereira, M. R. Correia, E. Pereira, K. P. O'Donnell, E. Alves, A. D. Sequeira, N. Franco, I. M. Watson and C. J. Deatcher: 'Strain and composition distributions in wurtzite InGaIn/GaN layers extracted from x-ray reciprocal space mapping', *Appl. Phys. Lett.*, 2002, **80**, (2002), 3913–3915.
121. S. V. Novikov, C. T. Foxon and A. J. Kent: 'Growth and characterization of free-standing zinc-blende GaN layers and substrates', *Phys. Status Solidi Appl. Mater. Sci.*, 2010, **207**, (6), 1277–1282.
122. D. As, D. Schikora, A. Greiner, M. Lübbers, J. Mimkes and K. Lischka: 'p- and n-type cubic GaN epilayers on GaAs', *Phys. Rev. B*, 1996, **54B**, (16), R11118–R11121.

123. C. T. Foxon, S. V. Novikov, N. M. Stanton, R. P. Campion and A. J. Kent: 'Free-standing zinc-blende (cubic) GaN substrates grown by a molecular beam epitaxy process', *Phys. Status Solidi*, 2008, **245**, (5), 890–892.
124. H. Yang, L. X. Zheng, J. B. Li, X. J. Wang, D. P. Xu, Y. T. Wang, X. W. Hu and P. D. Han: 'Cubic-phase GaN light-emitting diodes', *Appl. Phys. Lett.*, 1999, **74**, (1999), 2498.
125. T. Lei, T. D. Moustakas, R. J. Graham, Y. He and S. J. Berkowitz: 'Epitaxial growth and characterization of zinc-blende gallium nitride on (001) silicon', *J. Appl. Phys.*, 1992, (001), 4933–4943.
126. S. Li, J. Schörmann, D. J. As and K. Lischka: 'Room temperature green light emission from nonpolar cubic InGaNGaN multi-quantum-wells', *Appl. Phys. Lett.*, 2007, **90**, 10–13.
127. C. J. M. Stark, T. Detchprohm, S. C. Lee, Y. B. Jiang, S. R. J. Brueck and C. Wetzel: 'Green cubic GaInN/GaN light-emitting diode on microstructured silicon (100)', *Appl. Phys. Lett.*, 2013, **103**, (100).

Uncorrected Proofs